



ORAU TEAM Dose Reconstruction Project for NIOSH

Oak Ridge Associated Universities | Dade Moeller & Associates | MJW Corporation

Page 1 of 63

Document Title: Site Profile for the Stanford Linear Accelerator Center		Document Number: ORAUT-TKBS-0051 Revision: 01 Effective Date: 08/17/2007 Type of Document: TBD Supersedes: Revision 00
Subject Expert(s): N/A Site Expert(s): Norman D. Rohrig		
Approval:	<u>Signature on File</u> William A. Decker, Document Owner	Approval Date: <u>08/01/2007</u>
Concurrence:	<u>Signature on File</u> John M. Byrne, Task 3 Manager	Concurrence Date: <u>08/01/2007</u>
Concurrence:	<u>Signature on File</u> Edward F. Maher, Task 5 Manager	Concurrence Date: <u>08/01/2007</u>
Concurrence:	<u>Signature on File</u> Kate Kimpan, Project Director	Concurrence Date: <u>08/15/2007</u>
Approval:	<u>Brant A. Uish Signature on File for</u> James W. Neton, Associate Director for Science	Approval Date: <u>08/17/2007</u>

New
 Total Rewrite
 Revision
 Page Change

FOR DOCUMENTS MARKED AS A TOTAL REWRITE, REVISION, OR PAGE CHANGE, REPLACE THE PRIOR REVISION AND DISCARD / DESTROY ALL COPIES OF THE PRIOR REVISION.

PUBLICATION RECORD

EFFECTIVE DATE	REVISION NUMBER	DESCRIPTION
10/25/2006	00	New site profile document for Stanford Linear Accelerator Center to provide tables for dose reconstruction. First approved issue. Incorporates internal and NIOSH formal review comments. Responds to several A & A identified issues and completes TLD analysis. This revision results in no change to the assigned dose and no PER is required. Training required: As determined by the Task Manager. Initiated by Norman D. Rohrig.
08/17/2007	01	Revision 01 initiated to incorporate Attributions and Annotations section and additional references. Incorporates formal internal and NIOSH review comments. Changed Document Owner to William Decker due to a new COB issue explained in Section 7.0. Training required: As determined by the Task Manager. Initiated by William A. Decker

TABLE OF CONTENTS

<u>SECTION</u>	<u>TITLE</u>	<u>PAGE</u>
	Acronyms and Abbreviations	6
1.0	Introduction	9
1.1	Purpose	9
1.2	Scope	10
1.3	Site Profile Description	10
2.0	Site Description	10
2.1	Introduction	10
2.3	Radiation Characteristics	12
2.3.1	Electromagnetic Cascade	12
2.3.2	Activation Products and Internal Dose	13
2.3.3	External Fields from Activation	14
2.3.4	Beta Dose	16
2.3.5	Neutron Spectra	16
2.3.6	Synchrotron Radiation (SR)	19
3.0	Occupational Medical Dose	20
3.1	Introduction	20
4.0	Occupational Environmental Dose	20
4.1	Introduction	20
4.2	Internal Dose from Onsite Atmospheric Radionuclide Concentrations	21
4.2.1	Onsite Releases to Air	21
4.3	External Dose	21
4.3.1	Releases of Noble Gases and Short-Lived Positron Emitters	21
4.3.2	Ambient Radiation	22
4.3.3	Corrections on Environmental External Neutron Dose	24
4.4	Summary and Uncertainty	25
5.0	Occupational Internal Dose	26
5.1	Introduction	26
6.0	Occupational External Dose	27
6.1	Introduction	27
6.2	Basis of Comparison	28
6.3	Dose Reconstruction Parameters	29
6.3.1	Site Dosimetry Technology	29
6.3.1.1	RDC Film Badge	29
6.3.1.2	LiF TLD Disk System	29
6.3.1.3	Panasonic UD-802 System	30
6.3.1.4	Landauer Luxel System	30
6.3.2	Site Historical Administrative Practices	31
6.3.3	Calibration	32
6.3.3.1	Beta/Photon Dosimeters	32
6.3.3.2	Neutron Dosimeters	32
6.3.4	Workplace Radiation Fields	33

6.3.4.1	Beta/Gamma Dosimeter Response	33
6.3.4.2	Neutron Dosimeter Response	33
6.4	Adjustments to Recorded Dose (Including Neutron Weighting Factor).....	33
6.5	Missed Dose	35
6.6	Organ Dose.....	35
6.7	Uncertainty	36
7.0	Attributions and Annotations	36
	References	38
	Glossary.....	48
	ATTACHMENT A, HIGH-ENERGY THERMOLUMINESCENT NEUTRON DOSIMETRY	54

LIST OF TABLES

<u>TABLE</u>	<u>TITLE</u>	<u>PAGE</u>
2-1	Area information.....	11
2-2	Important radionuclides and other information from photoactivation of materials	14
2-3	Radionuclides generated by stray radiation from 28.5-GeV electrons on copper	15
2-4	Calculated saturated activity of radionuclides from photoactivated air	15
2-5	Common sources of exposure October to December 1998.....	15
4-1	Reported total activity released by year, primarily ⁴¹ Ar	21
4-2	Airborne release quantities	22
4-3	External neutron radiation 1972 to 1979.....	23
4-4	External neutron radiation 1980 to 1989.....	24
4-5	Net annual TLD photon doses at PMS locations	25
4-6	Neutron skyshine annual dose at different buildings	25
6-1	Historical doses.....	28
6-2	Recorded dose practices	31
6-3	Interpretation of reported data	31
6-4	Selection of beta and photon radiation energies and percentages.....	33
6-5	Measured neutron spectral quantities for facilities.....	34
6-6	Corrections for neutron dose based on detector energy dependence.....	34
6-7	Recommended IREP neutron energy fractions and correction factors.....	35
6-8	Missed dose.....	35
6-9	Conversion factors for organ dose.....	36
6-10	Uncertainty for neutrons.....	36
A-1	Measured and calculated response	58

LIST OF FIGURES

<u>FIGURE</u>	<u>TITLE</u>	<u>PAGE</u>
2-1	SLAC campus	11
2-2	Photon cross sections for copper.....	13
2-3	Calculated neutron spectra inside tunnel.....	17
2-4	Time-of-flight measured neutron spectra through iron and concrete	18
2-5	Neutron spectrum from 46.6-GeV electrons through iron and concrete	18
2-6	Neutron spectra at SSRL through 2 ft of concrete	19
4-1	Location of PMS detectors since 1983	24
A-1	Cross section versus neutron energy for some reactions of interest in neutron detection	55
A-2	Fluence and dose response vs. energy for PMS neutron detector	56
A-3	Log plot of dose equivalent/bin for high-energy neutron spectra and PMS instrument response	56
A-4	Albedo-neutron fluence integrated over the specified energy ranges vs. incident neutron energy for monoenergetic neutron fluences normally and isotropically incident on a 30-cm-thick semi-infinite tissue slab	60
A-5	Energy response of various albedo dosimeters.....	60
A-6	TLD response for monoenergetic neutrons	61
A-7	Sensitivity of TLDs versus moderated/unmoderated flux ratios with research area ratios inscribed.....	63

ACRONYMS AND ABBREVIATIONS

AEC	U.S. Atomic Energy Commission
Bq	becquerel
BSY	Beam Switch Yard
c	speed of light
CEDE	committed effective dose equivalent
CERN	European Organization for Nuclear Research
Ci	curie
cm	centimeter
CP	charge-parity
cpm	counts per minute
CR-39	Columbia Resin 39
ct	count
CY	calendar year
d	day
DAC	derived air concentration
DOE	U.S. Department of Energy
DOELAP	DOE Laboratory Accreditation Program
EEOICPA	Energy Employees Occupational Illness Compensation Program Act
ERDA	U.S. Energy Research and Development Administration
eV	electron-volt
ft	foot
g	gram
GBq	gigabecquerel
GeV	gigaelectron-volt, 1 billion electron-volts
GERT	General Employee Radiation Training
GM	Geiger-Mueller
GR	giant (electric dipole) resonance
GSD	geometric standard deviation
hr	hour
ICRP	International Commission on Radiological Protection
ICRU	International Commission on Radiation Units and Measurements
in.	inch
IREP	Interactive RadioEpidemiological Program
keV	kiloelectron-volt, 1,000 electron-volts
kg	kilogram
km	kilometer
kW	kilowatt
L	liter
LINAC	linear accelerator
LLD	lower limit of detection

m	meter
MeV	megaelectron-volt, 1 million electron-volts
mi	mile
min	minute
mm	millimeter
mR	milliroentgen
mrem	millirem
MRL	minimum reporting level
mSv	millisievert
mV	millivolt
n	neutron
nC	nanocoulomb
NCRP	National Council on Radiation Protection and Measurements
NECTA	Next Electron Collider Test Area
NIOSH	National Institute for Occupational Safety and Health
NOCTS	NIOSH OCAS Claims Tracking System
nrem	nanorem
NRTS	National Reactor Testing Station
NTA	nuclear track emulsion, type A
ODTS	Occupational Dose Tracking System
ORAU	Oak Ridge Associated Universities
PEP	Positron Electron Project
PEP-II	Positron Electron Project – II
POC	probability of causation
PMS	Peripheral Monitoring System
R	roentgen
RAMSY	Radioactive Material Storage Yard
RCA	radiologically controlled area
RDC	Radiation Detection Company
RWT	radiation worker trained
s	second
SLAC	Stanford Linear Accelerator Center
SLC	Stanford Linear Collider
SLD	SLC Large Detector
SPEAR	Stanford Positron Electron Asymmetric Ring
SRDB Ref ID	Site Research Database Reference Identification (number)
SSRL	Stanford Synchrotron Radiation Laboratory
Sv	sievert
TBD	technical basis document
TEDE	total effective dose equivalent
TEPC	tissue-equivalent proportional counter
TLD	thermoluminescent dosimeter
U.S.C.	United States Code
v	velocity
V	volt

yr	year
Z	atomic number
α	alpha particle
μm	micrometer
§	section

1.0 INTRODUCTION

1.1 PURPOSE

Technical basis documents and site profile documents are not official determinations made by the National Institute for Occupational Safety and Health (NIOSH) but are rather general working documents that provide historic background information and guidance to assist in the preparation of dose reconstructions at particular sites or categories of sites. They will be revised in the event additional relevant information is obtained about the affected site(s). These documents may be used to assist NIOSH staff in the completion of the individual work required for each dose reconstruction.

In this document the word “facility” is used as a general term for an area, building, or group of buildings that served a specific purpose at a site. It does not necessarily connote an “atomic weapons employer facility” or a “Department of Energy [DOE] facility” as defined in the Energy Employees Occupational Illness Compensation Program Act [EEOICPA; 42 U.S.C. § 7384l(5) and (12)]. EEOICPA defines a DOE facility as “any building, structure, or premise, including the grounds upon which such building, structure, or premise is located ... in which operations are, or have been, conducted by, or on behalf of, the Department of Energy (except for buildings, structures, premises, grounds, or operations ... pertaining to the Naval Nuclear Propulsion Program)” [42 U.S.C. § 7384l(12)]. Accordingly, except for the exclusion for the Naval Nuclear Propulsion Program noted above, any facility that performs or performed DOE operations of any nature whatsoever is a DOE facility encompassed by EEOICPA.

For employees of DOE or its contractors with cancer, the DOE facility definition only determines eligibility for a dose reconstruction, which is a prerequisite to a compensation decision (except for members of the Special Exposure Cohort). The compensation decision for cancer claimants is based on a section of the statute entitled “Exposure in the Performance of Duty.” That provision [42 U.S.C. § 7384n(b)] says that an individual with cancer “shall be determined to have sustained that cancer in the performance of duty for purposes of the compensation program if, and only if, the cancer ... was at least as likely as not related to employment at the facility [where the employee worked], as determined in accordance with the POC [probability of causation¹] guidelines established under subsection (c) ...” [42 U.S.C. § 7384n(b)]. Neither the statute nor the probability of causation guidelines (nor the dose reconstruction regulation) define “performance of duty” for DOE employees with a covered cancer or restrict the “duty” to nuclear weapons work.

As noted above, the statute includes a definition of a DOE facility that excludes “buildings, structures, premises, grounds, or operations covered by Executive Order No. 12344, dated February 1, 1982 (42 U.S.C. 7158 note), pertaining to the Naval Nuclear Propulsion Program” [42 U.S.C. § 7384l(12)]. While this definition contains an exclusion with respect to the Naval Nuclear Propulsion Program, the section of EEOICPA that deals with the compensation decision for covered employees with cancer [i.e., 42 U.S.C. § 7384n(b), entitled “Exposure in the Performance of Duty”] does not contain such an exclusion. Therefore, the statute requires NIOSH to include all occupationally derived radiation exposures at covered facilities in its dose reconstructions for employees at DOE facilities, including radiation exposures related to the Naval Nuclear Propulsion Program. As a result, all internal and external dosimetry monitoring results are considered valid for use in dose reconstruction. No efforts are made to determine the eligibility of any fraction of total measured exposure for inclusion in dose reconstruction. NIOSH, however, does not consider the following exposures to be occupationally derived:

- Radiation from naturally occurring radon present in conventional structures
- Radiation from diagnostic X-rays received in the treatment of work-related injuries

¹ The U.S. Department of Labor is ultimately responsible under the EEOICPA for determining the POC.

1.2 SCOPE

This Site Profile for the Stanford Linear Accelerator Center (SLAC) presents information useful for reconstructing doses received by SLAC employees.

Attributions and annotations, indicated by bracketed callouts and used to identify the source, justification, or clarification of the associated information, are presented in Section 7.0.

1.3 SITE PROFILE DESCRIPTION

This Site Profile contains tables that can be used to calculate the radiation dose received by a DOE contractor employee at SLAC. Section 2.0 discusses the site, the research that occurred there, and characteristics of the radiation exposure at SLAC. The radiation dose includes medical exposure from X-rays taken in the course of employment as discussed in Section 3.0. Section 4.0 covers the dose received from environmental pathways. Sections 5.0 and 6.0 discuss internal and external dose, respectively.

2.0 SITE DESCRIPTION

2.1 INTRODUCTION

The SLAC uses a 2-mi-long linear accelerator (LINAC) to accelerate electrons and positrons to extreme relativistic energies and uses these in high-energy physics experiments on the fundamental nature of matter.

Figure 2-1 shows the SLAC facility with many of the underground accelerators. The LINAC runs nearly west to east and crosses under Interstate 280 near the upper center of the picture. Most of the approximately 1,400 personnel work in the Central Laboratory area. SLAC researchers have received three Nobel prizes.

SLAC evolved from Project M (monster) at the Stanford University Physics Department. SLAC construction began in 1962 on the 420-acre site on the San Francisco peninsula about halfway between San Francisco and San Jose. Before and during construction at Stanford, some accelerator commissioning and testing of klystrons occurred. The first experiments occurred in 1966. Electrons were accelerated to 15 GeV in the 2-mi (3.2-km) linear accelerator bombarding fixed targets in end stations A, B, and C (near the center of Figure 2-1). End station C was replaced by various test beams.

The SLAC facility consists of several operational areas as listed in Table 2-1. As with most research facilities, the research program has evolved; new facilities have been added as new fields have been developed. The principal program at SLAC has been high-energy particle physics. Another significant program has been the use of synchrotron radiation from bending of the electron beams.

2.2 SITE ACTIVITIES

Positrons are initially produced in the positron vault near Sector 11 of the LINAC (the sectors are numbered from the source to the Beam Switchyard (BSY) from 1 to 30). In 1984 the positron source was moved to Sector 19. The accelerator energy was upgraded to 20 GeV by 1967, 33 GeV in 1980, and 50 GeV in 1987. In 1972, the small 3-GeV Stanford Positron Electron Asymmetric Ring (SPEAR) was built, beginning the use of particle colliders to increase the energy available for physics in the center of mass reference frame. In 1973, synchrotron radiation from the bends of SPEAR was used



Figure 2-1. SLAC campus (ESHD 2001, p 20 pdf).

Table 2-1. Area information.

Area	Description	Period	Access and shielding	Radioactivity Source	Radiation fields
LINAC Tunnel	2-mi (3.2-km) tunnel where LINAC accelerates electrons and positrons up to 50 GeV.	1966–2006	10 m underground, interlocked.	Air activation. Activated structures.	Electromagnetic cascade, GR neutrons.
Klystron Gallery	Hall above LINAC containing radio frequency power supplies (klystrons) that feed LINAC and provide acceleration.	1966–2006	Open. Klystrons wrapped in lead for X-ray shielding.	None	X-rays inside klystrons and leakage into gallery.
End Station A	Large experiment halls.	1966–2006	Interlocked.	Air activation.	Elementary particles,
End Station B	Beam dumps.	1966–2006	Thin roofs provide source for skyshine.	Activated structures.	electromagnetic cascade, neutrons.
End Station C		1966–1992			
BSY	Beam is directed to one of three end stations A, B, or C or to the PEP or SPEAR storage ring or linear collider SLC.	1966–2006	Interlocked.	Air activation. Activated structures.	
SPEAR SSRL	First storage ring used to study collisions between beam particles. Now used for synchrotron radiation experiments.	1972–2006	Interlocked hutches and storage ring.	Low-loss Non-issue	Intense photon source. Low-energy X-rays to infrared.

Area	Description	Period	Access and shielding	Radioactivity Source	Radiation fields
PEP & PEP-II	High-energy storage rings used for high-energy experiments. PEP-II is used as B factory.	1980–2006	Interlocked. Buried underground	Air activation. Activated structures.	
SLC	Linear collider using very small beams. Beam arcs buried 50-100 m underground.	1988–2006	Interlocked.	Air activation. Activated structures.	
Next Linear Collider Test Accelerator	Test bed for next linear collider.	1993–2006	Interlocked.	Air activation. Activated structures.	

for detailed imaging experiments in a wide variety of scientific applications using soft X-rays. The use of synchrotron radiation at the Stanford Synchrotron Radiation Laboratory (SSRL) to investigate forms of matter ranging from objects of atomic and molecular size to man-made materials with unusual properties attracts more than 1,600 researchers from 200 institutions every year (Stanford University 2006).

In 1980, the hexagonal Positron Electron Project (PEP) ring was constructed with six interaction regions where the two rings crossed. In 1984, damping rings were constructed near the injector (see Figure 2-1) to reduce the beam size and emittance, which increased the brightness and the rapidity of data accumulation. In 1988, the Stanford Linear Collider (SLC) was built with the SLC Large Detector (SLD). After the PEP research program was completed in 1982, the system was upgraded to PEP-II, which is used as a B factory to study charge-parity (CP) violation at the BaBar detector. An early description of the accelerator and research program is provided by Dupen (1966) and a later description is provided by Advman-Stoler (c. 1995). The accelerator area and the research yard are fenced off with access at the Sector 30 gate near the high-energy end of the LINAC or at a gate near SSRL. Dosimetry was required in the fenced area. In 1997, this requirement was reduced to only within Radiologically Controlled Areas (RCAs), which includes most open or office areas near an accelerator or beamline housing (Grissom 1997).

2.3 RADIATION CHARACTERISTICS

2.3.1 Electromagnetic Cascade

The electron and positron beams at SLAC (up to 50 GeV) are extremely relativistic (the beam energy now is about 100,000 times the electron rest energy), so when an electron interacts in a target material, an electromagnetic cascade develops. The absorption cross-section shape shown in Figure 2-2 for copper illustrates the different interaction processes that give rise to the photon spectrum (Vylet and Liu 2002, p 19). In the cascade process, high-energy electrons generate bremsstrahlung photons, which in turn generate electron and positron pairs via pair-production. This repeated bremsstrahlung and pair-production process is also called an electromagnetic shower. Electron-positron pairs are created in a shower that becomes thousands of times more intense over a distance of a few radiation lengths (distance for the mean particle energy to decrease by a factor of 1/e, about 6 mm in lead and 20 cm in concrete) into the material as the mean particle energy decreases. The radiation intensity decreases after the mean energy has dropped to a few MeV [see Figure 3-15 of the National Council on Radiation Protection and Measurements (NCRP) Report 144 for more information (NCRP 2003)]. An excellent description of the electromagnetic cascade is provided by Nelson (1987, p 155). Neutrons are generated by photon absorption, primarily from the giant (electric dipole) resonance (GR) leading to ~1 MeV neutron energies similar in spectrum to fission neutrons. Above

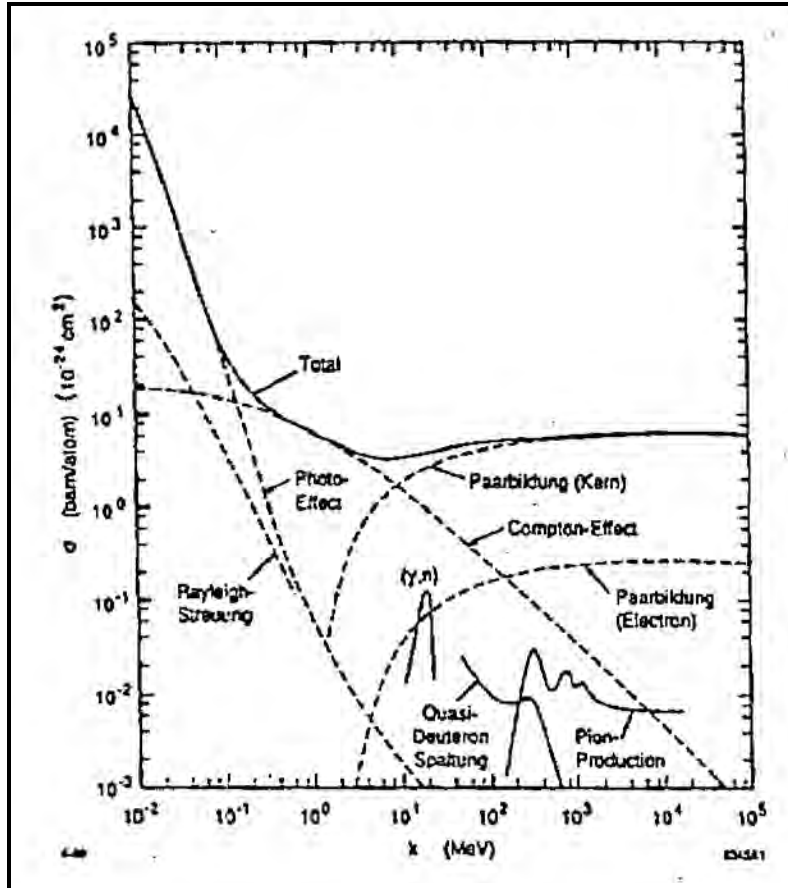


Figure 2-2. Photon cross sections for copper.

25 MeV, the quasi-deuteron reaction leads to intermediate-energy neutrons. Above 140 MeV, photopion production becomes possible, which leads to high-energy neutrons (100 MeV and above). Jenkins (1979) developed models for shielding for the photons and the three neutron energy groups.

2.3.2 Activation Products and Internal Dose

Neutron production and absorption leads to activation of the residual nucleus. Table 2-2 lists the nuclides generated in aluminum, steel, and copper struck by the electron or positron beam and the resultant cascade. Most of the worker dose comes from external exposure to these activated materials in maintaining the facility during beam-off time. The accelerator structure is activated to different radiation levels dependent on proximity to and intensity of the beam loss points (i.e., beam striking a structure).

The activation is retained in the structure of the accelerator. However, during the very occasional machining of these materials, inhalation of airborne nuclides is possible. Busick and Warren (1969, p7) compared the internal dose to the chemical toxicity and direct radiation and concluded that the internal dose is small. Donahue (1989², 1991, p 10) compared the possible internal dose to the external dose for a machining process and showed that the internal dose by this pathway is about 10^{-6} of the external dose (see the next to the last column of Table 2-2). Because external dose would be received during the setup of the machining process, the relative contribution from internal dose would be much smaller. These ratios depend on the assumed exposure and decay times, material mass

² The 1989 reference contains an error (cm vs m) that results in erroneous concentrations a factor of 10,000 larger.

Table 2-2. Important radionuclides and other information from photoactivation of materials (Donahue 1991).

Material	Isotope	Half-life	A(t) ^a (GBq/kW)	Concentration ^b (Bq/g)	Calculated concentration (DAC) ^c	ICRP 30 dose ratio ^d	ICRP 68 max. organ dose ratio ^d
Aluminum	Na-22	2.62 yr	2.1	10.0	9.1E-6	3.0E-7	2.4E-6 ET Airways
	Na-24	14.96 hr	3.4	15.9	2.1E-6		
	Be-7	53.6 d	4.7	21.8	7.4E-7		
Iron	Sc-46	83.9 d	7.0	0.37	1.0E-6	1.1E-7	5.3E-7 Spleen
	V-48	16.0 d	14.1	0.70	6.3E-7		
	Cr-51	27.8 d	14.1	0.78	2.6E-10		
	Mn-54	303 d	12.2	0.67	6.0E-7		
	Fe-53	8.2 hr	0.27	0.015	4.0E-10		
	Fe-55	2.60 yr	115	5.9	2.0E-6		
	Mn-56	2.58 hr	-- decay	--			
Copper	Co-58	71.3 d	23.3	13.0	1.3E-5	1.6E-6	3.1E-6 Lung
	Co-60	5.26 yr	3.0	1.70	5.0E-5		
	Cu-64	12.8 hr	50.3	27.8	8.3E-7		

a. Activity after 1-yr operation and 1-d cooling.

b. To give 1 mSv/hr at 30 cm from 10-cm-radius disc of 1 cm thickness.

c. Assumes typical machining operations on active materials; DAC = derived air concentration.

d. Ratio of internal dose from machining operation to external dose during machining, not including setup.

being machined, and detailed machining practices; however, the conclusion that internal exposure is trivially small in comparison to the external exposure remains true. These analyses were originally based on the methodology from International Commission on Radiological Protection (ICRP) Publication 30 (ICRP 1979) rather than the ICRP Publication 66 methodology (ICRP 1994) used for the EEOICPA program. They were redone to calculate the maximum organ dose for each material, and the dose to the most exposed organ provided in the last column of Table 2-2, is less than the external dose by at most a factor of 3×10^{-6} .

More recently, measurements with samples irradiated near a 90° angle in the accelerator tunnel with 28.5-GeV electrons hitting a copper beam dump for 3 days have identified the radionuclides listed in Table 2-3 (Rokni et al. 2001) produced from stray radiation. The agreement between Monte Carlo calculations and the measurements was generally within a factor of 2. The accelerator tunnel is activated to different levels depending on proximity to the beam loss points.

Some air activation occurs, which leads to the saturated activities for the nuclides listed in Table 2-4. The tritium activity is much less because saturation is not reached. During operation, the spaces where the activation occurs are not ventilated. Venting to reduce airborne exposure upon entry occurs through monitored vents after the beam is turned off and before the spaces are accessed (Jenkins, McCall, and Warren 1965).

2.3.3 External Fields from Activation

The intensity of the prompt radiation and induced activity is driven by the local beam losses, so it is quite high in targeting areas and low where the beam is efficiently transported. All beam-on high-radiation areas at SLAC are shielded and interlocked so that access is available only when the beam is off. The highest radiation fields are near the original positron production target near Sector 20 in the accelerator tunnel where the radiation field could be as high as 25 R/hr with the beam off. A 60-ft-long region of the accelerator tunnel near the positron-producing target, where the highest losses occur, is constructed of concrete loaded with glass frit to provide boron for neutron absorption, which results in a thermal capture mean free path of 1 inch to reduce radiation levels from activation

Table 2-3. Radionuclides generated by stray radiation from 28.5-GeV electrons on copper (Rokni et al. 2001).

	Material	Water	Aluminum	Iron	Copper	Soil
Total activity (Bq/g)		6.3	1.4	35	8.6	4.8
Isotope	Half-life	Fractional activity				
H-3	12.3 yr	0.10	0	0	0	0.06
Be-7	53.3 d	0.90	0	0	0	0.43
Na-22	2.6 yr	0	0.92	0	0	0.12
Sc-46	83.8 d	0	0	0.008	0.005	0.06
V-48	16.0 d	0	0	0	0	0.006
Cr-51	27.7 d	0	0	0.013	0	0.18
Mn-54	312.1 d	0	0.08	0.94	0.11	0.11
Fe-59	44.5 d	0	0	0.016	0.01	0.014
Co-56	77.3 d	0	0	0	0.04	0
Co-57	271.8 d	0	0	0	0.24	0
Co-58	70.8 d	0	0	0.019	0.42	0.009
Co-60	5.3 yr	0	0	0.006	0.16	0.005
Zn-65	244.3 d	0	0	0	0.01	0
Cs-134	2.1 yr	0	0	0	0	0.002

Table 2-4. Calculated saturated activity of radionuclides from photoactivated air (NCRP 2003).

Radionuclide	Half-life	Target element	Saturated activity (Bq/kW/m) ^a
H-3	12.3 yr	N, O	7.1E6
Be-7	54 d	N, O	1.1E6
C-11	20.5 min	N, O	1.1E7
N-13	10 min	N	1.1E10
O-15	2.1 min	O	5.6E7
Cl-38	37 min	Ar	6.8E5
Cl-39	55 min	Ar	8.5E6

a. Units are becquerels per kilowatt of beam power per meter of air through which the beam passes.

(DeStaeblers and Jenkins 1965). Other beam dumps also have fairly high radiation fields but are less than 1 R/hr. Table 2-5 lists common sources of exposure for the October to December 1998 period.

Table 2-5. Common sources of exposure October to December 1998 (Agot 1999, p 17).

Area	Component	Mrem/hr @ contact (historical)	Mrem/hr @ 30 cm	Max. contact radiation level encountered this quarter (mrem/hr)
BSY	D-10 Dump	2,000	80	100
	51 SL 1	2,000	20	100
	51 SL2	1,000	20	100
	51 D1	15,000	150	3,000
	52 D1	20,000	150	3,000
Beam Dump East	D-400 Dump	180	60	180
Damping Ring Injection Point & South Damping Ring	Ten-Finger Box	2,000	60	500
	PR-351	400	100	350
	Kickers	400	15	100
	Septums	1,000	30	400
North Damping Ring	Septums	1,600	25	200
	Kickers	600	5	40

Area	Component	Mrem/hr @ contact (historical)	Mrem/hr @ 30 cm	Max. contact radiation level encountered this quarter (mrem/hr)
N. Final Focus	Pc. 15	400		2
	Pc. 16.5	1,300		4
	TD-23	1,000		50
	Dump	30,000	150	2,200
S. Final Focus	ST-4	500		4
	PR-24	500		1
	TD-23	1,000		20
	C1X	500		80
	Dump	30,000	250	3,200
Positron Vault	Chicane	6,000	1,000	15,000
	Concentrator	1,000	100	2,000
	Target	400	80	4,000 o/s ^a
Sector 0, 2	Sec 0 chicane	500	30	500
	2-9 Dump	2,000	50	600
Sectors 19 & 20	Collimator EP01	900	200	200
	QF 204	800	150	2,000
Sectors 28, 29, 30	Collimator 29-9	1,500	100	1,000
	Collimator 29-1	2,000	400	1,800
PEP II Zone 8	HER Tune Dump	-	270	3,000
	LER Dump	-	10	80

o/s = out of service

2.3.4 Beta Dose

Because most of the activity is retained deep within the materials rather than at the surface, the beta dose is fairly small. McCall (1991, p119) calculated that the ratio of surface beta dose to gamma dose at 2.5 cm from the surface varied from 0.11 for iron to 0.31 for aluminum. Measurements of bare activated material with a survey meter by Busick and Dick (1991) with added absorbers in arrangements that emphasized the beta radiation showed the absorbed component was not measurable for a 100-mR/hr copper target, about 5% of the gamma for a 60-mR/hr iron target, about 32% for a 1.3-R/hr copper collimator, about 16% for a 16-mR/hr tungsten collimator, and about 54% for a 350-mR/hr aluminum and copper collimator. These are for bare activated material rather than material in a vacuum chamber that would absorb the beta radiation. Further measurements (Liu et al. 1995, p 75) with thermoluminescent dosimeters (TLDs), film, and an ion chamber at 10 SLAC field locations showed that the beta-photon ratio is in the range of 0.1 to 0.3. Therefore, the SLAC personnel external dosimetry program does not need to be accredited for beta radiation under the DOE Laboratory Accreditation Program (DOELAP) (Loesch 2004).

2.3.5 Neutron Spectra

Figure 2-3 shows the calculated neutron spectra inside the tunnel where Rokni et al. (2001) placed the water and soil samples for their activation study. The most intense peak is in the 1-MeV range, and there is a higher energy peak around 80 MeV. The water sample shows greater moderation than the soil sample, which is presumably because of the additional hydrogen (Rokni et al. 2001). The neutron spectra can be understood somewhat by considering the effects of shielding and scattering. Those in Figure 2-3 (generated with 28.5-GeV electrons) have essentially no shielding and show the characteristic GR peak about 1 MeV in energy. At 50 to 200 MeV, the high-energy neutrons are generated by the photopion process. Intermediate energy neutrons (10 to 20 MeV) from the quasi-deuteron process are between the two peaks, but Figure 2-3 does not show them. Scattered

neutrons all the way down to thermal energy levels are below the 1-MeV peak. Because this is a calculation, the vertical range is 4 orders of magnitude and the high-energy peak extends up to 700 MeV.

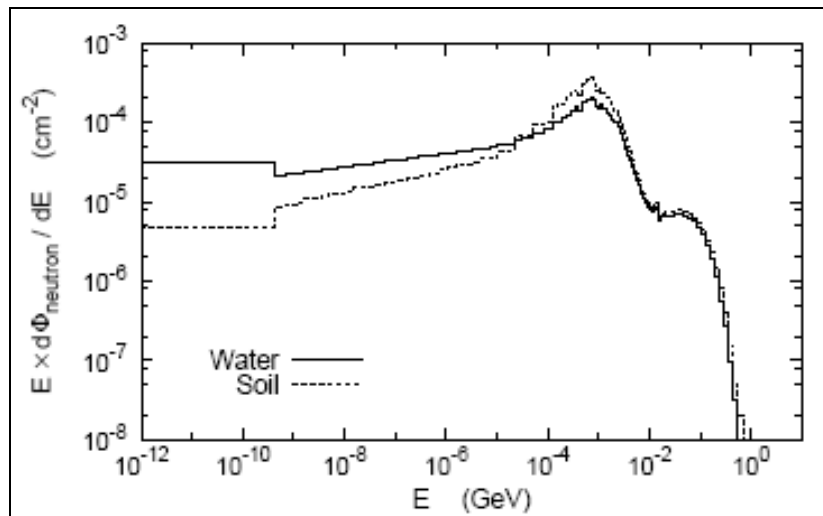


Figure 2-3. Calculated neutron spectra inside tunnel (Rokni et al. 2001).

Measurements of neutron spectra outside the concrete shielding have been performed but are complicated by the pulsed accelerator operation and the associated gamma burst when the beam hits the target. Figure 2-4 shows the high-energy portion of the neutron spectrum measured by time of flight from 28.7-GeV electrons at 90° to an aluminum beam dump through 84 cm (33 in.) of iron and the indicated thicknesses of concrete (Taniguchi et al. 2003, p 10). Figure 2-4 shows measurements and calculations made through very thick concrete (9 to 13 ft) of essentially the same source spectrum as in Figure 2-3. Because these are time-of-flight measurements, they do not extend below 6 MeV. Because of the thick shielding, the 1-MeV peak is no longer dominant, but a peak near 10 MeV from the quasi-deuteron process is becoming apparent.

Figure 2-5 shows the FFTB measurements with Bonner spheres and a ^{11}C detector (20-MeV threshold) in plastic scintillators to unfold the neutron spectrum. A specially modified 12-in.-diameter ball with a 1-cm-thick layer of lead was used to gain sensitivity to high-energy neutrons. This measurement system has been used in international intercomparisons at the European Organization for Nuclear Research (CERN) using a 30-GeV proton beam to characterize the field and to demonstrate measurement competence. The experiment was at an energy of 46.6 GeV and at a 16° angle downstream from the beam dump; the neutron dose rate was about 20 mrem/hr (Vylet et al. 1997). This equilibrium spectrum shows a clear peak near 1 MeV and 80 MeV with a slowing-down spectrum below 1 MeV. Because this is through thick shielding (4 ft of iron and 5 ft of concrete), the 1-MeV neutrons are comparable to the 50- to 80-MeV neutrons. The roughly $1/E$ spectrum from scattering below 1 MeV is typical and to be expected in such measurements.

Using the same technique, Figure 2-6 shows neutrons measured at SSRL. The SPEAR spectrum is at 90° for 2.3-GeV electrons striking a Faraday cup through 2 ft of concrete, and the LINAC spectrum is at 90° for 120-MeV electrons through about 2 ft of concrete. The high-energy peak is a small fraction in these spectra. With the thinner shielding, the 1-MeV peak is more prominent. The 120-MeV LINAC electron beam does not generate high-energy neutrons, so they are not in the spectrum. A few high-energy neutrons are generated at 2.3 GeV for the SSRL, but because the concrete is only 2 ft thick, the 1-MeV peak is the dominant peak.

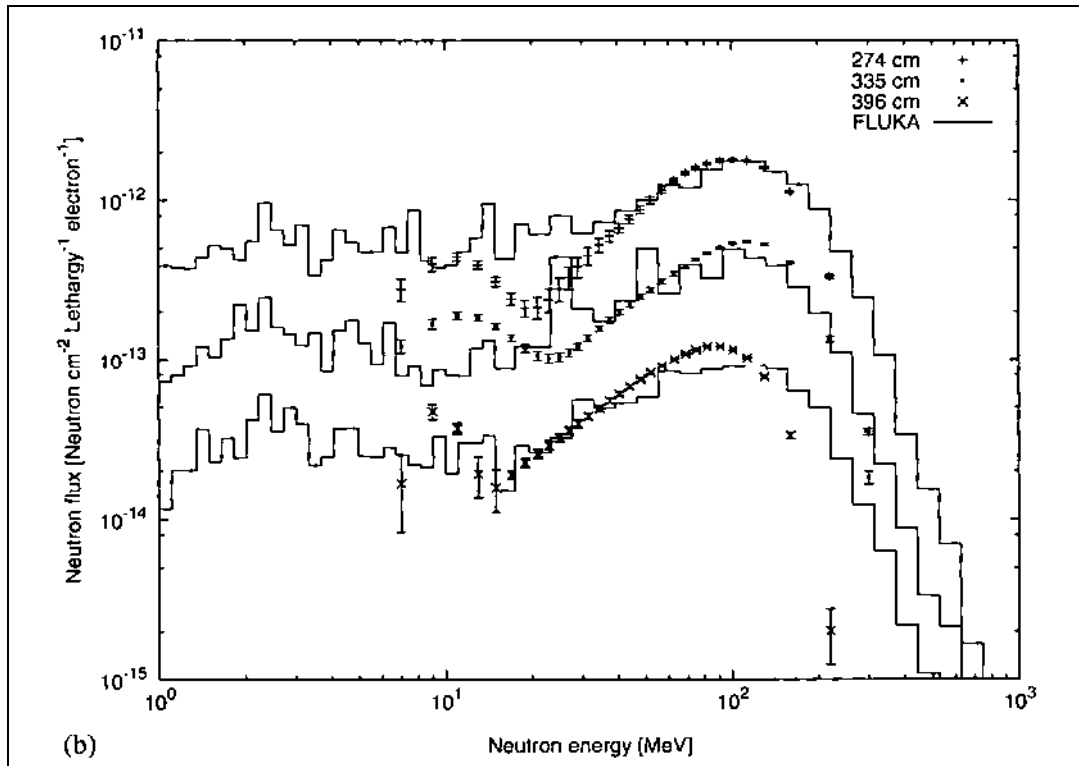


Figure 2-4. Time-of-flight measured neutron spectra through iron and concrete (Taniguchi et al. 2003).

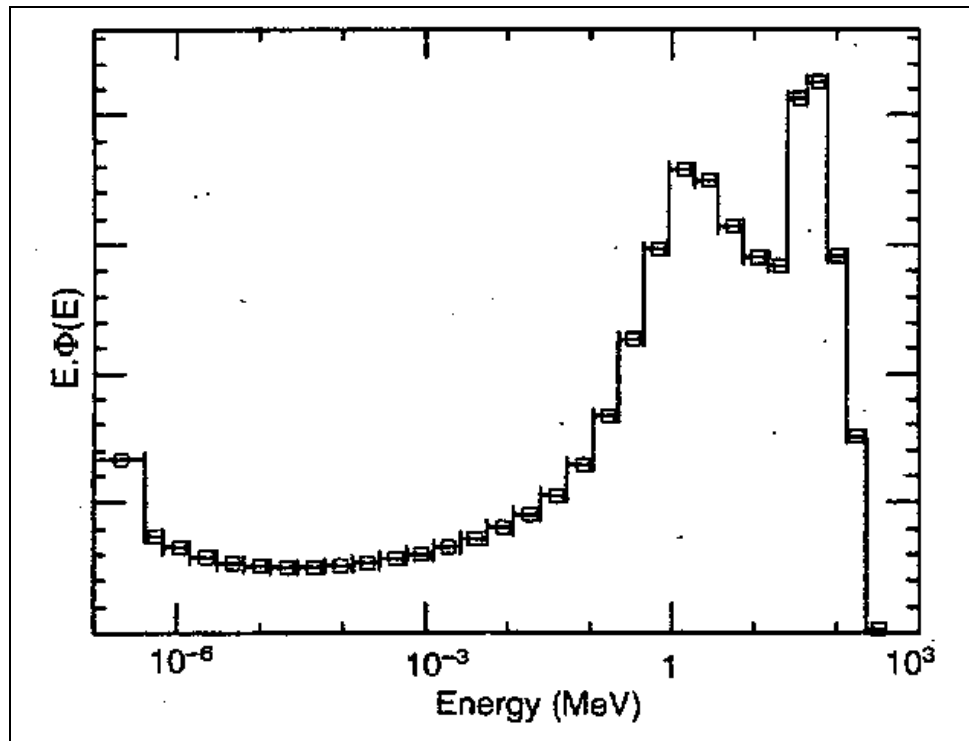


Figure 2-5. Neutron spectrum from 46.6-GeV electrons through iron and concrete (Vylet et al. 1997).

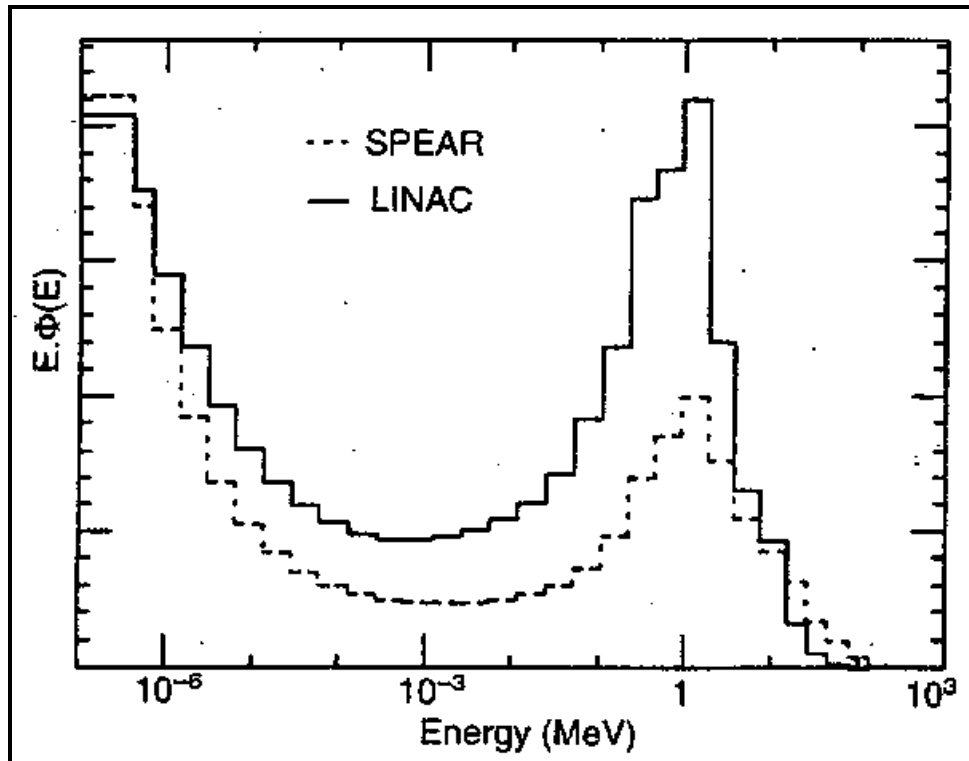


Figure 2-6. Neutron spectra at SSRL through 2 ft of concrete (Vylet et al. 1997).

Neutron spectra of concern for personnel exposure probably vary significantly. The skyshine exposures probably have a source similar to the lightly shielded SPEAR spectrum shown in Figure 2-6. For much of the SLAC experimental program, energies higher than 2.3 GeV were used, which would increase the high-energy component somewhat. To be detected at ground level, the skyshine must have at least one collision in the atmosphere, which would reduce the energy by a factor of about 2 on hydrogen but only by a few percent on oxygen and nitrogen (which comprise most of the elemental contents of air) (NCRP 1971, p 12).

The exposures in the research yard are a combination of skyshine and the leakage spectra, typically through fairly thick shielding similar to those used for Figure 2-5.

2.3.6 Synchrotron Radiation (SR)

Synchrotron radiation is formed when relativistic electrons or positrons are radially accelerated (i.e., bent) in a magnetic field. This can be a bending magnet or a special device such as a wiggler or an undulator where the beam is bent back and forth multiple times to enhance the radiation intensity. The continuous spectrum covering decades in energy range from a bend is characterized by a critical energy E_c with half the photon energy emitted above that energy and half below that energy (Margaritondo 1988, p 31). The critical energy depends on the electron energy and the magnetic field strength ($\sim BE^2$). SPEAR 3 operates at 3 GeV and has a bending magnet critical energy of 7.6 keV. SPEAR II operated at 3 GeV with a different magnet lattice and a critical energy of 4.8 keV. Above the critical energy, the flux falls with increasing energy exponentially as E/E_c (Weidemann 1998). Because synchrotron radiation is low energy, it scatters only weakly. The beamline hardware and hutches are designed to reduce SR levels to 0.05 mrem/hr (Liu et al. 2004a). The levels are generally less than 100 mrem/yr, which is fairly easy to accomplish and avoids training costs for many users [1].

In searches for the radiation field, a high-energy tail near the K-edge (88 keV) of lead, which is often used for shielding, is barely detectable. For the BL-11 wiggler with a monochromator, 68 keV photons dominate. For the white beam (no monochromator so full spectrum) the TVL is 1.7 mm of lead which applies for 150 keV photons (Liu et al. 2004b). The estimated photon spectrum in the area occupied by experimenters is 20% in the less-than-30-keV region and 80% in the 30- to 250-keV region. For purposes of dose reconstructions, it is favorable to claimants to assume that it is 100% in the 30- to 250-keV region. For any skin or eye doses exceeding the deep dose, these should be attributed to low energy photons.

3.0 OCCUPATIONAL MEDICAL DOSE

3.1 INTRODUCTION

Medical examinations for most DOE contractors usually involved chest X-rays. Such routine X-rays contribute dose that is included in the Interactive RadioEpidemiological Program (IREP) POC calculations. The SLAC medical department reports that it never gave such routine X-rays. Current medical documents do not identify chest X-rays as part of the examination process (Gherman 2006).

The analysis for this site profile examined SLAC record submittals for the EEOICPA claimants. As of March 2006, there were 27 EEOICPA claims for SLAC; the submittals vary in length from 3 to 345 pages with most being under 10 pages. The shorter ones did not contain any medical information. Seven claims were longer (from 36 to 345 pages) and appear to include the complete medical records of the claimants. The periodic medical examination record sheet has a space for X-rays and other medical tests such as blood pressure and pulse rate, but the X-ray indication was generally blank. The records included some X-rays taken in response to other medical conditions (such as a shoulder or an ankle functioning poorly), but these are outside the scope of the EEOICPA program. The analysis examined records for two other retirees that resulted in a similar conclusion.

U.S. Atomic Energy Commission (AEC) and U.S. Energy Research and Development Administration (ERDA) medical orders call for the performance of chest X-rays (AEC 1969, p 9; ERDA 1975). Because SLAC is part of Stanford University, it might not have followed the AEC requirements. SLAC began operations rather late (1962) for DOE contractors, which could account for it not providing routine X-rays. Early documents suggest that SLAC did not provide X-rays to employees (Freehafer 1964; Jenkins 1964a; Pindar 1965a; b). X-rays were given to beryllium workers (Pindar 1965b).

Based on this information, this analysis concludes that SLAC gave no X-ray examinations that EEOICPA dose calculations need to include.

4.0 OCCUPATIONAL ENVIRONMENTAL DOSE

4.1 INTRODUCTION

An unusual aspect of the environmental dose from SLAC is the contribution from skyshine neutrons from the target stations. Potential sources of internal and external dose from environmental pathways include (Busick 1972):

1. Short-lived gaseous releases from the accelerator tunnels based on calculations
2. Photon (gamma) radiation as measured by TLDs in recent years

3. Neutron radiation from skyshine near the target stations, which has been measured beginning in the early 1970s

4.2 INTERNAL DOSE FROM ONSITE ATMOSPHERIC RADIONUCLIDE CONCENTRATIONS

4.2.1 Onsite Releases to Air

The SLAC annual environmental monitoring reports contain estimates of air activity releases based on beam power, the air distance traversed, and access made to the beam areas. These releases are estimated for several areas (six in 1993 and nine in 2001) and for the short-lived nuclides listed in Table 2-4 and ^{41}Ar . Three nuclides (^{15}O , ^{13}N , and ^{11}C) are positron emitters and ^{41}Ar is an inert gas, so the only ones that contribute to internal dose are ^{38}Cl and ^{39}Cl . The chlorine ET airways (the maximum organ dose for chlorine) dose coefficients are very close [1.0×10^{-9} and 1.3×10^{-9} Sv/Bq respectively for 5- μm activity median aerodynamic diameter type M (ICRP 1995)], so it is reasonable to consider them together. In 1993, the calculated total release for chlorine was 0.36 Ci. Using a dispersion factor of 4.5×10^{-4} s/m³ for the site boundary at 400 m would result in an ET airways dose of about 0.053 mrem/yr. The site buildings are somewhat closer resulting in slightly larger doses, but still considerably less than 1 mrem/yr. Dose reconstructors can neglect such a small dose as a contributor to risk [background radiation is about 1 mrem/d (NCRP 1987)].

4.3 EXTERNAL DOSE

The external dose received in the environment consists of the prompt gamma and neutron radiation skyshine from the roofs of the facilities, primarily End Stations A and B, and the cloud gamma from released short-lived nuclides.

4.3.1 Releases of Noble Gases and Short-Lived Positron Emitters

When high-energy bremsstrahlung photons interact with room air, the short-lived isotopes listed in Table 2-4 are generated. Thermal neutrons generate ^{41}Ar with a 1.8-hr half-life. The accelerator tunnels in which these are generated are typically vented only after the beam is shut down and before personnel access. The early environmental monitoring annual reports state that the activity released was measured by monitors on the exhaust system and suggest that it is all from ^{41}Ar . The exhausts are at roof level without a stack. Table 4-1 lists the activities released from 1971 to 1985 as reported in the annual site environmental reports (Busick 1972; Busick and Holt 1973, 1974; HPS 1975 to 1980; RPHP 1981 to 1984; OHP 1985; ESO 1986). No releases were reported for 1986 to 1988 and 1998 (ESO 1987 to 1989; ESHD 1998b).

Table 4-1. Reported total activity (Ci) released by year, primarily ^{41}Ar .^a

Year	Total(Ci)	Year	Total(Ci)	Year	Total(Ci)
1971	5.2	1976	0.052	1981	1.1
1972	17.4	1977	1.7	1982	0.71
1973	6.1	1978	0.36	1983	0.44
1974	9.1	1979	1.7	1984	1.6
1975	13.6	1980	0.25	1985	0.138

a. Releases for 1986 to 1988 are reported as not measurable.

Beginning in 1989, the reports list calculated nuclide releases based on operational parameters rather than on measurements (see Table 4-2; ESO 1990; ESHD 1992a to 1998b, 2000, 2001, 2003,

2006a,b,c). Over the years, the calculations treated release parameters differently, which led to large inconsistencies because these nuclides are all short-lived.

Table 4-2. Airborne release quantities (Ci).

Year	Ar-41	O-15	N-13	C-11	Cl-38	Cl-39	Total (Ci)
1989		0.6	0.1	0.1			0.8
1990		1.8	0.38	0.42	0.021	0.042	2.7
1991	0.27	18.83	3.94	4.48	0.28	0.45	28.26
1992	0.21	14.72	3.08	3.52	0.22	0.35	22.11
1993	0.166	4.94E-4	0.358	1.20	0.133	0.229	2.09
1994	0.137	3.28E-17	1.01E-3	8.00E-2	NR ^a	NR	0.218
1995	6.4E-2	1.8E-2	5.4E-2	2.6E-1	NR	NR	0.4
1996	9.6E-2	1.2E-8	3.1E-2	3.0E-1	NR	NR	0.43
1997	7.8E-2	3.3E-2	1.4E-2	1.0E-1	NR	NR	0.23
1999	3.8	7.5	14.	1.9	NR	NR	27.0
2000	3.8	7.4	14.0	1.8	NR	NR	27.0
2001	4.7	9.1	17.0	2.3	NR	NR	33.0
2002	1.3	15.0	27.0	3.0	NR	NR	46.3
2003	1.1	12.0	24.0	2.9	NR	NR	40.0
2004	0.6	10	19	2.1	NR	NR	32

a. NR – Not reported

The associated doses from these nuclides are all very small. A CAP88 calculation that bounds these releases for a release of 100 Ci of ¹¹C at 150 m resulted in a maximum dose of 0.125 mrem/yr (Rohrig 2006a).

4.3.2 Ambient Radiation

When SLAC began operating, there was a program in place using eight Peripheral Monitoring Stations (PMS) to measure the prompt gamma and neutron fields near the site boundary using Geiger-Mueller (GM) counters and moderated BF₃ detectors, respectively (McCall and Jenkins 1966). These results are shown here as “mrem” to indicate that they require a calibration adjustment. Because of the higher natural gamma background, only neutron radiation was discernible from background. With counters, ambient dose levels (i.e., natural background) can be determined when the accelerator is off and compared to levels when the accelerator is operating. After 1990, high-sensitivity TLDs were used to monitor gamma radiation, and Columbia Resin 39 (CR-39) was used to measure the neutron fields. In the early years, area monitors were also used around the research yard, but results are available only for part of 1972 (fiscal year 1973) (Busick 1972). In 1972, all measured radiation fields in the research yard were less than 1 mrem/hr with one exception of less than 4 mrem/hr.

Data for 1966 to 1970 have not been found, although in 1968 a semi-annual report was expected (Rickansrud 1968). The 1971 document reports gamma plus neutron, which is not useful (Busick 1972). Table 4-3 lists the useful information from the PMS neutron detectors as reported in the 1972 to 1979 annual environmental reports (Busick and Holt 1973, 1974; HPS 1975 to 1980). The monitoring locations were on the site boundary at clock positions, relative to the LINAC beam direction, of approximately 1, 12, 11, 10, 9, 7, and 3 o'clock, respectively. Maps show PMS 7 is near the source of the LINAC where no neutrons are generated, and no values are ever given for that unit.

The active office buildings are between position 6 and End Station A (the principal skyshine source), and location 5 is the next nearest PMS to worker-occupied locations. Some systems were taken out of service for PEP construction. In the 1960s, operation was at lower power as systems were

developing. With storage ring and collider operation beginning in the 1970s, lower beam power was used, and beams were often not stopped in the large End Stations A and B.

Table 4-3. External neutron radiation 1972 to 1979 (“mrem”/yr)^a.

Year	PMS detector accelerator neutrons							Neutron background						
	1	2	3	4	5	6	8	1	2	3	4	5	6	8
1972	10.5	4.6	5.9	9.3	15.5	8.3	17.7	10.8	10.5	9.6	7.4	9.9	10.3	8.3
1973	3.1	1.5	3.2	3.9	4.9	0	4.5	8.1	8.1	8.1	8.1	8.1	8.1	8.1
1974	7.7	4.7	4.7	6.2	11.5	1.7	8.2	8.8	8.8	8.8	8.8	8.8	8.8	8.8
1975	8.8	2.4	4.8	oos	15.8	2	8.6	11.8	11.3	10.1		9.9	10.7	8.5
1976	1.8	nd	1.1	oos	3.4	nd	3.2	11.8	11.3	10.1		9.9	10.7	8.5
1977	5.2	2.1	oos	5.7	8.2	0.9	oos	12.8	11.2		9.6	10	10.8	
1978	oos	oos	oos	oos	6.6	0.8	oos					10	10.8	
1979	oos	oos	oos	oos	nd	nd	oos					10	10.8	

a. nd = not detectable (<1 mrem); oos = out of service.

Calibration of these detectors is presumed to have initially been to a PuF source with a mean energy of about 1.4 MeV. The first mention of the PuLi source is in 1985 (McCall 1985). Cosmic ray neutron background at sea level is about 2.6 mrem/yr (UNSCEAR 1988, p 52), which is significantly lower than the 8- to 12-mrem/yr background reported using these detectors.

In 1980 the locations of these systems were changed so that the new location 1 was in the old location 5. The locations are at 9, 10, 12, 2, 3, and 8 o'clock in relation to the LINAC beam direction, as shown in Figure 4-1. The results from these systems for 1980 to 1989 are shown in Table 4-4 (RPHP 1981 to 1984; OHP 1985; ESO 1986 to 1990). Many of the results were not detectable (about 1 mrem), and many systems were out of service due to SLC construction. In 1990 all units were out of service (ESHD 1992a).

“To supplement the PMSs for external photon and neutron dose monitoring, SLAC initiated an environmental thermoluminescent dosimeter (TLD) monitoring program near the end of the third quarter of calendar year (CY) 1991. Radiation Detection Company (RDC), a National Voluntary Laboratory Accreditation Program-certified dosimetry service, was contracted to provide SLAC with quarterly TLD dosimeters. The TLDs consist of two polyethylene capsules containing 30 mg each of ⁷LiF powder along with a CaSO₄:Dy dosimeter, which are heat sealed in an aluminized paper packet. Reproducibility levels (uncertainty values) of these environmental TLDs are within ±2 mR for CaSO₄:Dy and ⁷LiF, respectively” (ESHD 1992b, p 49) .

During the second quarter of CY 1992, SLAC expanded the TLD environmental monitoring program by adding two additional TLDs (i.e., models LDR-X9 and LDR-19) from Landauer Company. The LDR-X9 aluminum oxide TLD is designed to measure low-level photon radiation with a minimum detection level of 0.1 mrem (0.001 mSv). The LDR-19 is used for monitoring neutron dose with a minimum detection level of 10 mrem (0.1 mSv) (ESHD 1993, p 41). For CYs 1991 and 1992, all neutron and gamma TLD results were less than 1 mrem (ESHD 1992b, ESHD 1993). From 1993 to 2003, no neutron results were detectable.

Table 4-5 lists photon results from these systems (ESHD 1994 to 1998b, 2000, 2001, 2003). The 2002 results were compromised by inadequate attention to storage times (ESHD 2006a) and the 2003 and 2004 results were not reported (ESHD 2006b,c). The largest total dose for the 7 yr from 1995 to 2001 was 82.5 mrem at PMS6. This location is near LINAC Sector 20 (radiation from klystrons) far away from the site buildings. Dose reconstructors should assign a 3-mrem/yr photon dose based on the exposure for 2,000 (40 hr/wk for 50 weeks) of 8,766 hours that the TLDs were exposed (82.5 ÷ 7 × 2,000 ÷ 8,766).

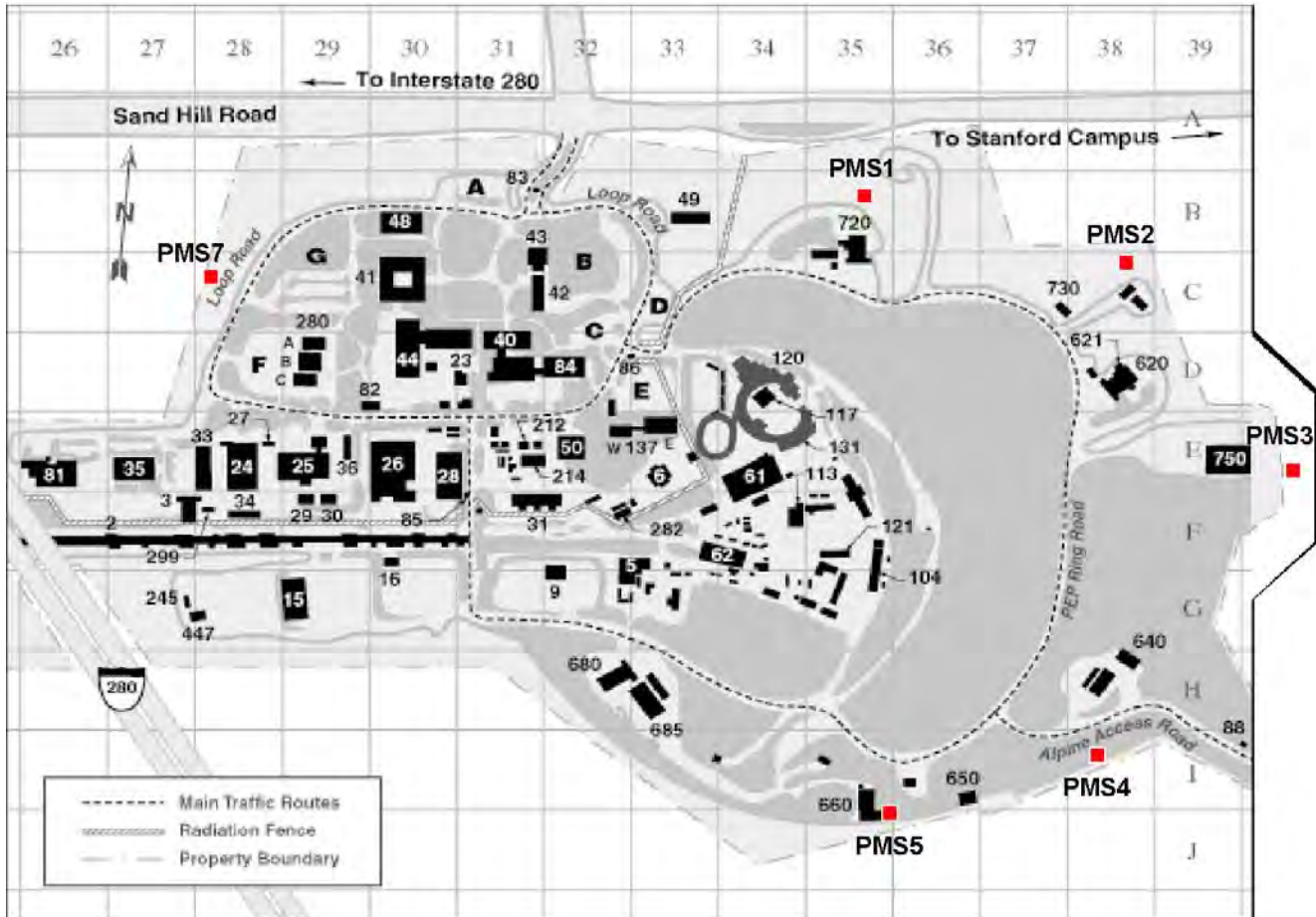


Figure 4-1. Location of PMS detectors since 1983. PMS 6 near Sector 20 is not shown on this map.

Table 4-4. External neutron radiation 1980 to 1989 (“mrem/yr”)^a

Year	PMS detector accelerator neutrons						Neutron background					
	1	2	3	4	5	7	1	2	3	4	5	7
1980	nd	nd	nd	nd	nd	nd	12	6.2	6.2	7.8	6.6	13
1981	nd	nd	nd	nd	nd	nd	12	12	12	15	12	13
1982	nd	nd	nd	nd	nd	nd	12	13	18	16	12	9.2
1983	5	nd	nd	nd	2	nd	13	11	14	16	12	10
1984	8	oos	oos	nd	5	nd	13	oos	oos	12	12	11
1985	6.7	oos	oos	oos	3	oos	13	oos	oos	oos	12	oos
1986	4.9	oos	oos	oos	1	oos	13	oos	oos	oos	12	oos
1987	2.1	oos	oos	oos	oos	oos	2.1	oos	oos	oos	oos	oos
1988	oos	oos	oos	oos	oos	oos	oos	oos	oos	oos	oos	oos
1989	1.2	oos	oos	oos	oos	oos	11.6	oos	oos	oos	oos	oos

a. nd = not detectable (<1 mrem); oos = out of service.

4.3.3 Corrections on Environmental External Neutron Dose

Two corrections must be made for the environmental neutron dose. The first corrects for the energy dependence of the neutron detector as shown in Attachment A, Figure A-1. Following the discussion in Attachment A, the neutron doses need to be multiplied by 1.51 ± 0.53 . The second corrects for the well-known distance dependence of the skyshine field.

Table 4-5. Net annual TLD photon^a doses (mrem) at PMS locations.

Year	PMS1	PMS2	PMS3	PMS4	PMS5	PMS6	PMS7
1993	7.7	-9.0	5.2	0.2	-1.9	22.4	NR ^b
1994	0.6	0.0	1.7	0.0	1.7	11.1	NR
1995	2.2±5.8	3.1±6.0	4.4±5.6	2.0±6.0	1.5±5.8	4.2±5.8	5.4±5.7
1996	11.1±6.2	1.2±5.9	5.8±5.9	1.9±6.1	3.1±6.0	15.1±6.3	8.1±5.8
1997	8.4±7.1	8.0±8.1	-2.1±5.8	-5.4±6.1	-2.3±6.8	6.6±6.6	2.1±6.5
1998	14.2±6.3	5.7±6.0	13.7±7.2	6.4±5.9	7.3±6.4	16.7±6.0	8.1±6.2
1999	12.5±6.1	5.0±6.1	7.8±6.2	1.9±5.6	0.5±6.0	14.8±6.4	1.1±5.8
2000	11.4±6.2	8.0±6.0	15.0±6.6	3.5±6.1	11.4±6.1	12.1±7.5	3.2±5.8
2001	11±6	9±6	14±6	0±6	4±5	13±7	4±5

- a. All neutron doses for 1993 to 2004 are "Below Minimum Detection Levels" (20 mrem).
 b. Not reported.

Jenkins (1974) demonstrated that a function of the form:

$$H(r) = H(r_0) \frac{r_0}{r} e^{-\frac{(r-r_0)}{140m}} \tag{4-1}$$

describes the distance dependence of the radiation field for neutron skyshine from the SLAC accelerator. This function is used to estimate doses in buildings. Based on distances from End Station A (the primary source of skyshine through the years), adjustment factors on the PMS dose from station 1 (previously 5) range from 0.6 to 2. The dose rate at PMS1 when it was not detectable was taken as 1 "mrem"/yr. Estimates for the early years were generated by extrapolation from the 1972 values. Estimates for the later years when TLDs were used were based on the latest years of monitor operation. The PMS doses were based on 8,766 hr of exposure. Doses applied for dose reconstruction should be based on 2,000 hr (40 hr/wk for 50 weeks), so the above values should be multiplied by 0.228. Combining all three corrections and grouping the buildings by distance, the calculated neutron skyshine dose by year is provided in Table 4-6. If a person's work location is unknown, dose reconstructors should use the maximum value provided in the second column.

4.4 SUMMARY AND UNCERTAINTY

SLAC has monitored environmental dose throughout its history. Radioactivity releases have been so small as to not lead to significant occupational environmental dose. Skyshine radiation (primarily from neutrons) contributes the doses shown in Table 4-6. A calibration uncertainty of 35% was assigned to this component. Estimates of the annual dose from photon radiation skyshine are more uncertain. Measurements of photon skyshine haven't been as productive. Assignment of an annual photon dose of 3 mrem as discussed above Table 4.5 is recommended. This value should be assumed to encompass the critical uncertainty range. Dose reconstructors should not add these doses if the energy employee was monitored.

Table 4-6. Neutron skyshine annual dose (mrem) at different buildings.

Year	Buildings							
	Maximum	137, 86, 50	31, 214, 84	85, 40, 42	26, 44	82	41	280, 48, 25
1966	6	6	5	4	3	2	2	2
1967	7	7	6	5	3	3	2	2
1968	8	8	7	6	4	3	3	2
1969	10	10	9	7	5	4	3	3
1970	11	11	10	7	5	4	4	3
1971	11	11	10	7	5	4	4	3
1972	11	11	10	7	5	4	4	3

Year	Buildings							
	Maximum	137, 86, 50	31, 214, 84	85, 40, 42	26, 44	82	41	280, 48, 25
1973	3	3	3	2	2	1	1	1
1974	8	8	7	6	4	3	3	2
1975	11	11	10	8	5	5	4	3
1976	2	2	2	2	1	1	1	1
1977	6	6	5	4	3	2	2	2
1978	5	5	4	3	2	2	2	1
1979	1	1	1	0	0	0	0	0
1980	1	1	1	0	0	0	0	0
1981	1	1	1	0	0	0	0	0
1982	1	1	1	0	0	0	0	0
1983	3	3	3	2	2	1	1	1
1984	6	6	5	4	3	2	2	2
1985	5	5	4	3	2	2	2	1
1986	3	3	3	2	2	1	1	1
1987	1	1	1	1	1	1	1	0
1988	2	2	2	1	1	1	1	1
1989	1	1	1	1	0	0	0	0
1990–2005	3	3	2	2	1	1	1	1

5.0 OCCUPATIONAL INTERNAL DOSE

5.1 INTRODUCTION

As an electron accelerator laboratory, SLAC does not generate significant removable radioactivity; most of the radioactivity is deep within the structure of the materials that stopped beam particles. Earlier analyses (Busick and Warren 1969; Donahue 1991) demonstrated that the committed effective dose equivalent from machining activated materials would be much less than the external exposure (Table 2-2). Examination of the claimant files did not identify any reports of internal dose measurements. DOE has accepted the position that internal exposure is highly unlikely, so a DOELAP-accredited bioassay program in this area is unnecessary (Muhlestein 2001). For the principal isotopes generated at SLAC, (^3H , ^{22}Na , ^{46}Sc , ^{54}Mn , ^{55}Fe , and ^{60}Co) the highest organ dose is 1 to 10 times the effective dose equivalent and most of it is delivered in the first year after the intake.

The SLAC internal dosimetry technical basis document (Kase et al. 1993; Tran 2005) indicates that a conventional internal bioassay program is unnecessary because workers are unlikely to receive a committed effective dose equivalent of 100 mrem/yr from internal activity. This conclusion was based on analysis of swipe data, airborne radioactive materials, exposure to activated water, and exposure during torching of activated materials.

Between 1993 and 2004, only 317 positive swipes were recorded for removable radioactive material. Most of these were on individual items rather than for areas of the facility. Only three (at 25,000, 50,000, and 100,000 cpm) exceeded 10,000 cpm on a pancake GM counter, 32 were between 1000 and 10,000 cpm, and 282 were under 1000 cpm, all from contamination areas (Tran 2005, p 10). The airborne activity levels document (Sit 2000) demonstrates that the highest smear, if applicable to large areas, would result in inhaled doses less than 10 mrem for a 1-d exposure. This analysis is predicated on the assumption that the sample was all ^{54}Mn , which has a low derived air concentration (DAC) and is hard to detect with a pancake probe. The procedure requires that, if the threshold activities in Sit (2000) are exceeded, the sample would be analyzed with a gamma spectrometer, which would then allow use of isotope-specific DAC values in the evaluation. Where there is any question, respirator use is usually required. Air-sampling results on job activities have resulted in a

negligible signal above a contemporary radon background measurement (Gooch 2005). Air samples are taken near but outside the work area prior to work to get a radon background result. Air sample results are then compared to these results until the radon has been allowed to decay, after which they are compared to instrument background.

To demonstrate that induced airborne radioactivity is not an issue, high-volume air samplers were used in the accelerator housing. High-efficiency membrane filters were examined using a shielded germanium detector, and no detectable radioactivity was found on any of the samples. Sample volumes greater than 21,000 L were collected from the accelerator housing immediately after accelerator shutdown (Kase et al. 1993; Tran 2005).

Radioactive iron (7.2 kg) reading 60 mrem/hr (contact) was cut with a torch for 15 min, and air samples were collected. Measured activities (primarily ^{54}Mn and ^{60}Co) corresponding to 0.007 to 0.03 times the DAC were found on the three air samples, and the operator sample showed 0.09 DAC (Busick 1992). Because 1 DAC-hr corresponds to 2.5 mrem, such an extreme condition would result in only 0.06 mrem committed effective dose equivalent (CEDE) based on ICRP Publication 30 methodology (ICRP 1979). Table 2-2 showed that the internal exposure to the most exposed organ is about 3×10^{-6} of the external exposure for a machining operation not considering setup.

An individual was thoroughly wetted inadvertently with water from a Low Conductivity Water System, used for facility cooling, that contains tritium (Allan 2004). A very conservative assumption that the wetting was similar to drinking 2.2 L of water (0.05 L might be more realistic) resulted in an ICRP CEDE of 0.0016 mrem.

SLAC has active air-sampling and contamination control programs, which have found that no one has been internally contaminated. The SLAC has an agreement with Lawrence Livermore National Laboratory for whole-body counting, which can detect isotopes of concern if the need arises (Muhlestein 2001).

Based on these considerations, no internal dose should be assigned for all SLAC employees unless an intake is identified in the worker files.

6.0 OCCUPATIONAL EXTERNAL DOSE

6.1 INTRODUCTION

Since the beginning of construction, SLAC has provided radiation dosimeters to appropriate individuals. All individuals entering the accelerator area have been required to wear radiation dosimeters. The initial film badges, which were provided by RDC, used nuclear track emulsion, type A (NTA) film for neutron radiation and probably Kodak Type 2 film for gamma radiation.

The SLAC design dose limit was initially 500 mrem based on an extrapolation by Dr. Wolfgang K. H. (Pief) Panofsky (the first SLAC director) of regulatory dose limits over time to when SLAC would be operating. Measured doses have generally been less than 1 rem as shown in Table 6-1.

With the advent of TLDs, SLAC developed a TLD reader and used LiF TLD disks purchased from Teledyne for what it called an accident dosimeter system. The disks were mounted in a card that could be carried in the worker's wallet or worn on a clip. Neutron dose was based on the difference between the ^6LiF and ^7LiF disks. The system did not use cadmium covers, so it was overly sensitive to thermal neutrons and albedo neutrons.

Table 6-1. Historical doses

Year	Collective dose(rem)	Collective neutron dose(rem)	# with measurable dose	Average measured dose (mrem)	# with <100 mrem	# with 100-500 mrem	# with >500 mrem	Max dose (mrem)
1969	11.14	1.55				63	1	<600
1970	21.31	0.68				54	15	<1,500
1971						50	18	<1,500
1972	30			150	1,368	146	23	<3,000
1973	23			120	1,753	65	9	<3,000
1974	16			82	1,649	67	10	<3,000
1975	16			81	162	23	2	<1,000
1976	9.4			47	173	11	3	<750
1977	13			62	176	10	1	<1,000
1978	9			54	161	24	2	<1,000
1979	4.9			24	174	11	2	<1,000
1980	3.3			18	175	12	0	<500
1981	3.6			21	179	8	0	<500
1982	5.4			29	175	10	2	<750
1993	44.1	7.4	521	77	101	96	8	999
1994	17.5	2.9	235	74	49	47	2	894
1995	25.6		304	84	75	72	3	769
1996	17.583		269	65	38	4	1	644
1997	13.847		105	132	38	1	3	996
1998	12.684	0.141	144	71				
2002	3.607	0.496	99	36				
2004	3.798	0.04	108	35				

With the development of DOELAP, SLAC tested the LiF system and then moved to the more conventional UD-802 automatic TLD system manufactured by Panasonic, which became DOELAP accredited. Neutron signal was based on the difference between the natural lithium borate and calcium borate TLDs., The SLAC prompt photon dose is from photons with energies at the cross-section Compton minimum at a few MeV, The induced isotopes, which dominated the personnel doses, also emit photons at more than a few hundred keV. Therefore, the sensitivity difference at low energy caused by different Z for the two TLD materials is unimportant.

In late 1997, SLAC reduced the badging requirements to only those areas defined as RCAs (Stanford University 2005) where radiation doses above 100 mrem in a year are likely or where contamination is possible (Grissom 1997). Workers are still encouraged to wear their badges while at work, even when not in an RCA. However, in actual implementation, most areas with doses even much less than 100 mrem/y are still classified as the RCAs.

In 2002, SLAC implemented a DOELAP-accredited Landauer Luxel commercial dosimetry system.

Throughout the history of SLAC, the record contains several references to dosimeters not being returned.

6.2 BASIS OF COMPARISON

The standard for comparison of deep doses is the personal dose equivalent at a 1 cm depth introduced in International Commission on Radiation Units and Measurements (ICRU) Report 47 (ICRU 1992). This quantity was used directly in the DOELAP process, and adjustments to it for previous times should follow standard EEOICPA processes. For the lens of the eye and skin dose,

which are extremely rare at SLAC, a depth of 3 mm and a tissue density of 7 mg/cm², respectively, should be used. For neutrons, corrections are provided to calculate the ambient dose equivalent using the tables in ICRP Publication 74 (ICRP 1996).

6.3 DOSE RECONSTRUCTION PARAMETERS

6.3.1 Site Dosimetry Technology

6.3.1.1 RDC Film Badge

Jenkins (1964b) lists detection criteria and error tolerances. The minimum reporting level (MRL) was 10 mrem for gamma and 30 mrem for neutrons. NTA film was used for neutron radiation, and Kodak Type 2 film was used for gamma radiation. Based on the number of fields counted (25 at 25 power), 50 mrem is probably a more realistic MRL for the NTA film. This system was used through June 1971. The filter arrangement is believed to be a multi-element system similar to that reported in 1995 for a field characterization study (Liu et al. 1995). Such a multielement system was used at the National Reactor Test Station beginning in 1958 (Cipperley 1968).

Collective dose information is available for 1969 and 1970 (Author unknown 1971); the gamma dose totals were 11,140 and 21,310 mrem, respectively. In 1969, 16 persons had positive neutron doses (10 greater than 20 mrem) with a total of 1,550 mrem. In 1970, five persons had neutron doses totaling 680 mrem.

6.3.1.2 LiF TLD Disk System

SLAC constructed a TLD reader using a ¹⁴C-based stabilized light source for standardization (McCall 1969, Svensson, McCall, and Babcock 1970). TLD disks of 0.4-mm-thick LiF with a diameter of 12.7 mm for ⁷Li and 12 mm for ⁶Li from Teledyne were used as detectors. The badges were embedded in plastic similar to a credit card. All SLAC employees were assigned one of the accident detectors that was to be carried in the wallet. Radiation workers (about 200) were on a quarterly exchange; all others were on an annual exchange. The badge was shown to the guard when the accelerator area was entered.

In 1987, the stated MRL was 20 mrem for gamma and neutron radiation (Jenkins and Busick 1987); in 1995, it was 20 mrem (Grissom 1995). In July 1995, the lower limit of detection (LLD) for the system was determined through measurement and calculation by the DOELAP formula as 7 mR for photons and 18 mrem for neutrons; the LLD was officially stated as 10 mR for photons and 20 mrem for neutrons (Sit 1995).

The neutron dose based on the difference between the ⁶Li and ⁷Li TLD results is calculated as 1 mrem/nC in comparison to the gamma dose as 1 mrem/nC. The TLDs are not shielded with cadmium, so they also detect thermal neutrons (Jenkins and Busick 1987).

In 1978, 287 workers had reported neutron doses above 20 mrem, with all but 35 under 80 mrem and the highest under 230 mrem. Busick (1981) noted that these were probably overestimated by approximately 100%. In 1993 and 1994, the collective doses were 44.1 and 16.3 person-rem with 16.8% and 16.4% neutrons, respectively (Grissom 1995).

Application was made for DOELAP accreditation in March 1986 (Rickansrud 1986), and the performance testing was completed in 1986 (Gesell 1986) and repeated in 1992 (Carlson 1992). With the advent of the DOE Radiological Control Manual (DOE 1994), the annually badged worker

population was called General Employee Radiation Training (GERT) trained and the quarterly badged worker population was called Radiation Worker Training (RWT) trained.

Backgrounds were measured at SLAC employee homes and varied from 8.5 to 15.2 mrem in 115 d or a spread of about 21 mrem in a year (Flood 1995a).

6.3.1.3 Panasonic UD-802 System

Beginning in January 1996 (Flood 2000a), the Panasonic system was used. This system uses four TLDs to unfold responses for high-energy gamma, low-energy gamma, beta, and neutrons and reports a shallow, a lens, and a deep dose equivalent. The TLDs used are lithium tetraborate (LiBO) or $\text{Li}_2\text{B}_4\text{O}_7\text{:Cu}$ and calcium sulfate (CaSO) or $\text{CaSO}_4\text{:Tm}$. The phosphors are only about 10 mg/cm^2 thick and the Li and B are natural, so ^6Li should only be about 7.4% of the Li and ^{10}B should be only about 20% of the B. The photon signal on the $\text{Li}_2\text{B}_4\text{O}_7\text{:Cu}$ is subtracted based on the $\text{CaSO}_4\text{:Tm}$, which has a higher Z, which will affect the low-energy photon response and thus complicate photon signal subtraction. The system performed acceptably when tested with M30 X-rays.

As part of the DOELAP accreditation, the deep dose LLD was determined by measurement and calculation for the Panasonic UD-802 dosimeter for seven different combinations of low- (M150) or high-energy (^{137}Cs) photons and low- (moderated ^{252}Cf) or high-energy (^{252}Cf) neutrons (Flood 1995a). The LLD for individual radiations and photon mixture results were between 10 and 13 mrem, high-energy photons and high-energy neutron mixtures resulted in 15 mrem, and low-energy photons and high-energy neutron mixtures resulted in 35 mrem. Because of the higher Z, the low-energy photon response is higher for CaSO_4 than for $\text{Li}_2\text{B}_4\text{O}_7$, and the natural lithium neutron response is lower than ^6LiF TLDs, which results in the larger LLD. In 1997 the LLD was revisited to consider a neutron signal in the background and to calculate an LLD for deep and shallow dose equivalents. The LLD for low-energy photons and high-energy neutron mixture is 70 mrem (Flood 1997). The MRL used for dosimetry reporting is 20 mrem for neutron and gamma both annual and quarterly (Flood 1995a, Flood 1995b, Flood 1997).

6.3.1.4 Landauer Luxel System

The annual GERT badges switched for CY 2002 to the Landauer Luxel Type P system, which does not include a neutron dosimeter. The quarterly RWT badges, which were switched during the last quarter of CY 2002, use the Luxel Type J system containing CR-39, which is used for neutron dosimetry. The Luxel badges use aluminum oxide (Al_2O_3) in a sealed packet that is sandwiched into a special filter pack with rapidly varying thickness (like a very small egg carton). For exposures greater than 500 mrem, the irradiation pattern on the detector can be examined; if the badge was stationary, the pattern from the filter will be sharp, but if the badge moved in the field as if worn by a person, the pattern will be washed out. Neutron radiation of the CR-39 damages the material. The material is then chemically etched to make the proton recoil tracks visible, and they are counted to determine the dose. The system was DOELAP-accredited in 2002 and again in December 2004 in categories I-IV, VI, and VII (Loesch 2004). The badge LLD is advertised at 0.1 mrem, but background variations noted above in the SLAC area are much larger than that (study repeated in 2002 with similar results). The LLD calculated for DOELAP irradiations was 0.15 mrem for photon deep dose and 6.4 mrem for neutron deep dose (Tran 2004a). With a 10-mrem MRL for the annual badge, the collective dose to the GERT group would be 2.448 rem rather than the 0.825-rem collective dose with a 20-mrem MRL (Frey 2003). The MRL was set at 10 mrem for quarterly badges and 20 mrem for annual badges (Frey 2003; Tran 2004b).

6.3.2 Site Historical Administrative Practices

Recorded dose practices are summarized in Table 6-2, and interpretation of reported data is provided in Table 6-3. The early dosimeter results from RDC were provided on computer-generated paper reports issued after the badge exchange. Summary reports were prepared quarterly and annually. The DOE responses to dose requests in the claimant files show a simple statement such as, "Dose records from 1970-1973 (about [some number] mrem) were obtained from copies of personal dose reports." Copies of several of the dose reports are on the Oak Ridge Associated Universities (ORAU) Team network O-drive. Reported dose in millirem for the period is divided into nonpenetrating (beta) and penetrating in two categories (neutron and X + gamma). Cumulative penetrating and nonpenetrating doses are provided in millirem for the quarter and the year. Lifetime records for penetrating and nonpenetrating doses are provided in rem in 1961, but in millirem in 1971.

Table 6-2. Recorded dose practices [2].

Year	Dosimeter measured quantities	Compliance dose quantities
RDC Multielement beta/photon film dosimeter + NTA neutron dosimeter		
10/1961–6/1971	X or gamma Beta Neutron	Penetrating = gamma + neutron
LiF TLD		
7/1971–1995	Gamma Neutron	Total = gamma + neutron
Panasonic UD-802 TLD System		
1996–2002	Beta Lens of eye Gamma Neutron	Total = gamma + neutron
Landauer Luxel Type J–Quarterly		
Oct 2002–2006	Beta Gamma Neutron	Total = gamma + neutron
Landauer Luxel Type P–Annual		
2002–2006	Beta Gamma	Gamma

Table 6-3. Interpretation of reported data [3].

Period	Reported quantity	Interpretation of zeroes	Interpretation of blanks (no data)	Monitored/unmonitored
1961–6/1971	mrem	Default entry	Not issued	G in col 5 means dosimeter not issued
7/1971–1995	mrem	<MRL	Not measured	
1996–2002	mrem	<MRL	Not measured	
2003–2006	mrem	<MRL	Not measured	

Records from 1974 to the present are provided from the Occupational Dose Tracking System (ODTS) in a printout generated when the request is received. Each badge results in 1 line of output, with a line after each year for total effective dose equivalent (TEDE). There are columns for skin dose, lens of eye dose, photon/deep dose, neutron dose, total dose, left hand, right hand, left foot, right foot and CEDE.

In ODTS, the skin dose and lens dose columns are blank when the LiF system was used because they were not measured. The reported total dose is the sum of the neutron and photon/deep doses. The annual TEDE is the sum of the badge total doses.

In the Panasonic years, the algorithm generated the first four dose categories. A zero value indicates the result is less than the MRL.

6.3.3 Calibration

6.3.3.1 Beta/Photon Dosimeters

SLAC has a gamma well in Building 24 that has had the same ^{137}Cs source in it since 1967 (Tran 2006). Since 1990, the fields have been measured with a Radcal set of calibration chambers (Radcal 1991). Before that, they were probably measured with Victoreen R chambers.

The commercial photon dosimeters have been calibrated by the vendors. The RDC film badge system presumably used a ^{226}Ra source, a ^{137}Cs source, or a ^{60}Co source free in air without a phantom but with charged particle equilibrium. These would be referenced to the National Institute of Standards and Technology and calibrated to exposure in roentgen.

The LiF system used a ^{60}Co and ^{137}Cs source for calibration free in air without a phantom but with charged particle equilibrium. The testing in the late 1980s of this system with DOELAP would have involved irradiations on phantom.

The Panasonic system is calibrated with ^{137}Cs free in air without a phantom but with charged particle equilibrium using the new C_x . Irradiations using the standard DOELAP conditions were provided by Pacific Northwest National Laboratory.

The Landauer system is presumed to be calibrated using the DOELAP protocols.

6.3.3.2 Neutron Dosimeters

SLAC has used five types of neutron sources in calibrations of the LiF TLD system and the Panasonic UD-802 system. Two PuBe sources were purchased in September 1963, PuB and PuF sources were purchased in July 1966, and two more PuBe sources were purchased in April 1977 (MCC 1977). SLAC also has a PuLi source that was apparently purchased in 1981³ and one or more ^{252}Cf sources (Liu et al. 1991). However, the reported neutron dose equivalent for the LiF system has been tied to the signal from a gamma source (^{60}Co or ^{137}Cs). A reported 1 millirem neutron dose will generate the same light in the Li F TLD as 1 mrem of gamma dose. Reported responses for this system vary from 0.45 V/mrem for PuBe calibration to 150 V/mrem for thermal neutrons (Liu et al. 1991).

Dose using the Panasonic system was defined from the response to the moderated ^{252}Cf source. Beginning in March 2000 (Flood 2000b), in consideration of the high-energy neutron peak at 80 to 100 MeV, the dose conversion factors were divided by 2, which effectively doubled the reported neutron dose equivalent. Without additional information, this analysis assumed that, between 1996 and March 2000, the Panasonic system used the dose response for a moderated ^{252}Cf neutron source generated by the Tennessee Valley Authority (Colvett, Gupta, and Hudson 1988). The energy dependence of the Panasonic is the same as that for the LiF system.

The Landauer CR-39 system marketed as Neutrak 144 has been tested against several monoenergetic sources at the Radiological Research Accelerator Facility (Columbia University) and Tohoku University (Tran 2004b), and it is calibrated against the DOELAP standard. The detector is sensitive above a few tens of keV; it responds to radiation damage from proton and heavy ion recoils. Dose reconstructors should assume that neutrons below 50 keV are not detected.

³ Liu et al. (1991) references a 1981 "Information Sheet for Neutron Source" from the Savannah River Site that has not been found. It is assumed that this reference is for the PuLi source. That source is also referred to in McCall (1985) and McCall (1988) references, but not earlier.

6.3.4 Workplace Radiation Fields

6.3.4.1 Beta/Gamma Dosimeter Response

Beta radiation is comparatively less significant than gamma radiation because it is almost always stopped by the surrounding material. In the rare cases when the innards of a piece of activated hardware are accessible, the beta radiation as noted in Section 2.3 is only 10% to 30% of the gamma field at the same location.

The gamma radiation fields at SLAC are due to activation nuclides and machine operation. The electromagnetic shower from the primary beam results in photon energies in the few MeV region. X-ray radiation from the klystrons is in the 300- to 400-keV range. Synchrotron radiation is in the less-than 30-keV energy range, but extends to higher energies. There may be a small amount of electromagnetic shower from beam losses. The radiation dosimeters used at SLAC should reliably measure all photons. These fields are classified according to the IREP codes in Table 6-4. EEOICPA default values should be used for minor adjustments to make to the recorded photon dose.

Table 6-4. Selection of beta and photon radiation energies and percentages [4].

Process	Description/ buildings	Operations		Radiation type	Energy (keV)	Percentage
		Begin	End			
Klystron galleries and klystron maintenance shop	Amplify microwave power to accelerate beam and repair klystrons.		1965	2006	Beta	100
	34	30-250			50	
		>250			50	
Calibrations	Site calibration of instruments and dosimeters		1965	2006	Beta	100
	24	30-250			25	
		> 250			75	
SSRL	Synchrotron radiation		1973	2006	Beta	NA
	120, 131, 650, 730				photon	100
High Energy Physics Area	Electromagnetic cascades		1966	2006	Beta	100
	61, 62, 9, 750, 620, 640, 660, 680, 720	30-250			10	
		> 250			90	
Maintenance	Induced activity		1966	2006	Beta	100
		30-250			25	
		> 250			75	

6.3.4.2 Neutron Dosimeter Response

Attachment A discusses the neutron dosimeter response in the prevailing fields at SLAC and the development of the correction factors in Tables 6-6 and 6-7.

6.4 ADJUSTMENTS TO RECORDED DOSE (INCLUDING NEUTRON WEIGHTING FACTOR)

Corrections must be made to the neutron doses because the neutron dosimeters did not respond to the entire spectrum of neutrons and because the IREP standard for neutron exposure does not include the quantities measured by SLAC. Table 6-5 contains the neutron spectral data from SLAC and divides the dose into the IREP dose intervals. The table also shows the fractions of dose below 50 keV and 800 keV and the nominal energy thresholds for the CR-39 and NTA neutron detectors for each measurement. Table 6-6 contains these factors as well as the corrections for the TLD systems.

The calculated adjustments to convert neutron dose equivalent to ambient dose are shown in Table 6-7 for each spectrum so that organ doses can be calculated using Appendix B of the *External Dose*

Table 6-5. Measured neutron spectral quantities for facilities [5].

Process	Description	Operations		Neutron energy	NCRP 38 ^a	Ambient dose
					dose fraction (%)	equivalent / dose equivalent
SSRL injector	SSRL LINAC 2 ft concrete 120-MeV electrons	1990	2006	<10 keV	0.062	1.01
				10–100 keV	0.029	1.13
				0.1–2 MeV	0.593	1.36
				2–20 MeV	0.299	1.10
				>20 MeV	0.018	0.89
				<0.8 MeV	0.386	
				<0.05 MeV	0.075	
High-energy physics area	SSRL SPEAR 2 ft concrete 2.3-GeV electrons	1972	2006	<10 keV	0.074	1.06
				10–100 keV	0.018	1.12
				0.1-2 MeV	0.417	1.36
				2–20 MeV	0.392	1.09
				>20 MeV	0.099	0.84
				<0.8 MeV	0.289	
				<0.05 MeV	0.082	
High-energy physics area	FFTB2 4 ft iron, 5 ft concrete 46.6-GeV electrons	1966	2006	<10 keV	0.013	0.92
				10–100 keV	0.009	1.09
				0.1–2 MeV	0.206	1.28
				2-20 MeV	0.310	1.03
				>20 MeV	0.463	0.67
				<0.8 MeV	0.120	
				<0.05 MeV	0.016	

NCRP (1971).

Table 6-6. Corrections for neutron dose based on detector energy dependence.^a [6]

Time interval	Detector system	Issue	Impact	Total impact
1961–6/1971	NTA Film Badge	Insensitive below 800 keV	Lose 12-40%	Multiply by 1.53 ±0.14
		Not detect heavy recoils	Lose 30-40 % of 50-2%	
7/1971–1995	LiF Albedo TLD	Conservative reporting	Divide by 1.8 with GSD of 2.5	Multiply by 0.56 GSD of 2.5
1996–3/2000	Panasonic TLD	Use unmoderated rather than moderated Cf for dose evaluation	Divide by 7. GSD of 2.5	Multiply by 0.14. GSD of 2.5.
		Not measure high-energy neutrons	Lose 2-50 %	
4/2000–2001	Panasonic TLD		May overcompensate for high-energy neutrons.	None GSD of 2.5.
2002–2005	Landauer CR-39	Insensitive below 50 keV	Lose 1.6-8%	Multiply by 1.12 ±0.04
		Not detect heavy recoils	Lose 30-40 % of 50-2%	

GSD = geometric standard deviation.

Reconstruction Implementation Guideline (NIOSH 2002). The conversion for neutrons above 20 MeV from measured doses to ambient dose is less than 1 because the dose equivalent at 1 cm depth for the ambient dose is less than deep dose. The conversions from ambient dose equivalent to organ dose are generally greater than 1 because of this condition (NCRP 1971, App. B). Conversions from deep dose equivalent to organ dose are not available above 20 MeV (NIOSH 2002).

Table 6-7. Recommended IREP neutron energy fractions and correction factors.^a [7]

Process	Description	Operations		Neutron energy	Default	Ambient	Net
					dose (%)	dose equiv/dose equiv	correction factor
Instrument calibration	Alpha Be source calibrations Cf-252 source calibrations	1962	2006	0.1-2 MeV	20	1.4	0.28
				2-20 MeV	80	1.1	0.88
SSRL injector	SSRL LINAC Skyshine	1990	2006	<10 keV	0.06	1	0.06
				10-100 keV	0.03	1.1	0.033
				0.1-2 MeV	0.60	1.4	0.84
				2-20 MeV	0.30	1.1	0.33
				>20 MeV	0.02	1.0 ^b	0.02
High-energy physics area	SSRL SPEAR Thin shielding	1972	2006	<10 keV	0.08	1	0.08
				10-100 keV	0.02	1.1	0.22
				0.1-2 MeV	0.40	1.4	0.56
				2-20 MeV	0.40	1.1	0.44
				>20 MeV	0.10	1.0 ^b	0.10
High-energy physics area	FFTB2 Thick shielding	1966	2006	<10 keV	0.01	1	0.01
				10-100 keV	0.01	1.1	0.011
				0.1-2 MeV	0.20	1.4	0.28
				2-20 MeV	0.30	1.1	0.33
				>20 MeV	0.50	1.0 ^b	0.50

a. Multiply the corrected recorded neutron dose equivalent by the net correction factor to obtain the ambient dose equivalent in each IREP energy interval.

b. The conversion of 1.0 is used based on the OTIB-55 recommendation for neutron energies greater than 20MeV..

6.5 MISSED DOSE

The missed dose for SLAC dosimetry systems is identified in Table 6-8 based on the EEOICPA standard practice of MRL/2 for each badge with a zero result. This is not a very large factor because SLAC went to quarterly and annual dosimeter cycles as early as 1971. After the missed dose is determined, the corrections from Tables 6-6 and 6-7 need to be applied.

Table 6-8. Missed dose [8].

Period of use	Dosimeter	Photon MRL ^a (mrem)	Neutron MRL ^a (mrem)	Exchange frequency	Annual missed photon dose (mrem) ^b	Annual missed neutron dose (mrem) ^b
1962-June 1971	Film-RDC	10	50	Monthly	60	300
			50	2 weeks	130	650
July 1971-1995	LiF TLD homemade system	20	20	Quarterly	40	40
July 1971-1995			20	Annual	10	10
1996-Sept 2002	UD-802 Panasonic TLD	20	20	Quarterly	40	40
1996-2001			20	Annual	10	10
Oct 2002-2006	Landauer Luxel	10	10	Quarterly	20	20
2002-2006	OSD	20	NA	Annual	10	NA

a. Estimated MRLs for each dosimeter technology in the workplace.

b. Maximum annual missed dose calculated using MRL/2 from NIOSH (2002, p 16).

For cancers affected by beta dose, it will be favorable to the claimant to assume a beta dose for years between 1971 and 1996 of 30% of the gamma dose received by the worker (see § 2.3.4).

6.6 ORGAN DOSE

To determine the organ dose, the dose conversion factors in Table 6-9 should be used.

Table 6-9. Conversion factors for organ dose [9].

Period	Photon dose conversion factor	Neutron dose conversion factor
1961-1996	Exposure to organ	Ambient dose equivalent to organ
1996-2006	H _{p,10} to organ	Ambient dose equivalent to organ

6.7 UNCERTAINTY

For photons, dose reconstructors should use the default biases and uncertainties appropriate for the different periods. For neutrons, the biases should be corrected as described in Section 6.4. The uncertainty factors are stated in Table 6-10.

Table 6-10. Uncertainty for neutrons [10].

Site-specific dosimetry system	Uncertainty factors
Film-RDC	0.30
LiF TLD homemade system	GSD of 2.5
UD-802 Panasonic TLD	GSD of 2.5
Landauer Luxel OSD	0.30

7.0 ATTRIBUTIONS AND ANNOTATIONS

Where appropriate in the preceding text, bracketed callouts have been inserted to indicate information, conclusions, and recommendations to assist in the process of worker dose reconstruction. These callouts are listed in this section with information that identifies the source and justification for each item. Conventional references are provided in the next section that link data, quotations, and other information to documents available for review on the ORAU Team servers.

Norman Rohrig served as the initial Document Owner of this document and had no Conflict or Bias with SLAC when this document was written. On April 3, 2007, Mr. Rohrig informed the ORAU Team that he had accepted employment with SLAC which created a Conflict or Bias for the SLAC site. As a result, he was replaced as Document Owner by William Decker. Mr. Rohrig continues to participate on the Document Team in the role of Site Expert in compliance with the NIOSH Conflict or Bias policy.

- [1] Rohrig, Norman D. ORAU Team. Health Physicist. April, 2006.
While discussing skyshine calculations and measurements from End Station A with Stan Mao (SLAC Health Physicist), it was apparent that the primary driver for shield design was that the radiation levels in SSRL be less than 100 mrem in a year. In addition, the SSRL is not identified in the RCA listing on the Web page (Stanford 2005).
- [2] Rohrig, Norman D. ORAU Team. Health Physicist. April, 2006.
This standard TBD table is based on information in Section 6.3.1 and its references.
- [3] Rohrig, Norman D. ORAU Team. Health Physicist. April, 2006.
This standard TBD table is based on information in Section 6.3.1 and 6.3.2 references and the dose reports.
- [4] Rohrig, Norman D. ORAU Team. Health Physicist. April, 2006.
This standard TBD table is based on information in the site profile references, Section 2.3.1, and Figure 2-2.

- [5] Rohrig, Norman D. ORAU Team. Health Physicist. April, 2006.
This standard TBD table is based on information in Section 2.3.5 combined with standard dose conversion factors.
- [6] Rohrig, Norman D. ORAU Team. Health Physicist. April, 2006.
This standard TBD table is based on information in Attachment A.
- [7] Rohrig, Norman D. ORAU Team. Health Physicist. April, 2006.
This standard TBD table is based on information in Table 6-5.
- [8] Rohrig, Norman D. ORAU Team. Health Physicist. April, 2006.
This standard TBD table is based on information in Section 6.3.1.
- [9] Rohrig, Norman D. ORAU Team. Health Physicist. April, 2006.
This standard TBD table is based on information in Section 6.3.1.
- [10] Rohrig, Norman D. ORAU Team. Health Physicist. April, 2006.
This standard TBD table is based on information in Attachment A and an understanding of error propagation.
- [11] Rohrig, Norman D. ORAU Team. Health Physicist. April, 2006.
The right-hand side shows the response per unit dose equivalent which is determined by dividing the response per unit fluence by the dose conversion factor.
- [12] Rohrig, Norman D. ORAU Team. Health Physicist. April, 2006.
The PMS response is that shown in Figure A-2 on a logarithmic scale. The neutron spectra are from Section 2.3.5 and are multiplied by the dose conversion factor.
- [13] Rohrig, Norman D. ORAU Team. Health Physicist. April, 2006.
The correction is based on the ratio of the counts per nanorem for the PuF calibration spectrum and the SSRL LINAC spectrum for the PMS. Because the PMS will have a smaller response to the FFTB2 spectrum, using it would result in a larger dose by the factor $0.385/0.135$. The uncertainty is taken as the ratio of the calculated sensitivities for two measured fields (the CERN iron and CERN concrete spectra) and the ratio of the measurements. The measurements (10 and 1.8) are provided in Table A-1. The calculated results are in Rohrig (2006b) worksheet CERN Spect in cells U40 and AA39.
- [14] Rohrig, Norman D. ORAU Team. Health Physicist. April, 2006.
The correction factor of 1.8 with a GSD of 2.5 provides a range of 0.72 to 4.5, which is somewhat larger than the range of 0.75 to 4 in the previous paragraph.

REFERENCES

- AEC (U.S. Atomic Energy Commission), 1969, "Chapter 0528, Occupational Health Program," *AEC Manual*, Washington, D.C., December 5. [SRDB Ref ID: 4644]
- Advman-Stoler, N., C. 1995, *A Brief History of SLAC: An Introduction to the Stanford Linear Accelerator Center*. [SRDB Ref ID: 23307, p. 228]
- Agot, W. L. 1999, "4th Quarter 1998 Rad Worker Permit (RWP) Supplemental Dosimeter Exposure Summary for SLAC Employees", memorandum to S. Frey and B. Flood, Stanford University, Stanford Linear Accelerator Center, Stanford, California, February. [SRDB Ref ID: 23235, pp. 13–17]
- Allan, J., 2004, "PS-20 Water Release," memorandum to S. Rokni et al., Stanford University, Stanford Linear Accelerator Center, Stanford, California, September 2. [SRDB Ref ID: 23199]
- Alsmiller, R. G. Jr., and J. Barish, 1974, "The Calculated Response of ⁶LiF Albedo Dosimeters to Neutrons with Energies ≤ 400 MeV," *Health Physics*, volume 26, pp. 13–28. [SRDB Ref ID: 25414]
- Author unknown, 1971, "Notes on cost of badging and dose distribution", Stanford University, Stanford Linear Accelerator Center, Stanford, California. [SRDB Ref ID: 23216]
- Busick, D. D., 1972, *Annual Environmental Monitoring Report, January – December, 1971*, SLAC-154, Stanford University, Stanford Linear Accelerator Center, Stanford, California. [SRDB Ref ID: 23150]
- Busick, D. D., 1981, "Letter McCaslin to Warren, December 18, 1980," letter to Joe McCaslin (Lawrence Berkeley Laboratory), Stanford University, Stanford Linear Accelerator Center, Stanford, California, January 7. [SRDB Ref ID: 23166, p. 14]
- Busick, D., 1992, "Safety Analysis Memo for Airborne Radioactivity," revised memorandum, Stanford University, Stanford Linear Accelerator Center, Stanford, California, October 15. [SRDB Ref ID: 23307, p. 522]
- Busick, D., and B. Dick, 1991, "Results of Absorption Measurements from Irradiated Targets and Gamma to Beta Emission Ratio," revised memorandum to M. Grissom and G. Warren, Stanford University, Stanford Linear Accelerator Center, Stanford, California, October 29. [SRDB Ref ID: 23283]
- Busick, D. D., Holt, E., 1973, *Annual Environmental Monitoring Report, January – December, 1972*, SLAC-159, Stanford University, Stanford Linear Accelerator Center, Stanford, California. [SRDB Ref ID: 23152]
- Busick, D. D., Holt, E., 1974, *Annual Environmental Monitoring Report, January – December, 1973*, SLAC-170, Stanford University, Stanford Linear Accelerator Center, Stanford, California. [SRDB Ref ID: 23157]
- Busick, D. D., and G. J. Warren, 1969, *Operational Health Physics Associated with Induced Radioactivity at the Stanford Linear Accelerator Center*, SLAC-PUB-696, Stanford University, Stanford Linear Accelerator Center, Stanford, California, December. [SRDB Ref ID: 21518]

- Cipperley, F. V., 1968, *Personnel Dosimetry Standard Operating Procedure Effective March 30, 1958*, IDO-12070, U.S. Atomic Energy Commission, Idaho Operations Office, Idaho Falls, Idaho, December. [SRDB Ref ID: 8086]
- Carlson, R. D., 1992, "DOELAP Performance Test", DOELAP Performance Evaluation Program Administrator letter to M. Grissomm (Stanford Linear Accelerator Center), August 18. [SRDB Ref ID: 25384]
- Colvett, R. D., V. P. Gupta, C. G. Hudson, 1988, "TVA's Dose Algorithm for Panasonic Type 802 TLDs," *Radiation Protection Management*, volume 5, pp. 49–62. [SRDB Ref ID: 23307, p. 348]
- DeStaebler, H., and T. Jenkins, 1965, *Pu-Be Neutron Measurements in the Accelerator Tunnel*, SLAC-TN-65-24, Stanford University, Stanford Linear Accelerator Center, Stanford, California, March. [SRDB Ref ID: 23378]
- DOE (U.S. Department of Energy), 1994, *U.S. Department of Energy Radiological Control Manual*, DOE/EH-0256T, Rev. 01, Office of Assistant Secretary for Environment, Safety and Health, Washington, D.C., April. [SRDB Ref ID: 14856]
- Donahue, R. J., 1989, "Calculation of Internal Radiation Exposures at a High-Energy Electron Accelerator," *Radiation Protection Dosimetry*, volume 29, pp. 189–194. [SRDB Ref ID: 23307, p. 486]
- Donahue, R. J., 1991, *Calculation of Internal Radiation Exposures at a High-Energy Electron Accelerator*, SLAC-PUB-4941, Rev. 2, Stanford University, Stanford Linear Accelerator Center, Stanford, California, January. [SRDB Ref ID: 21367]
- Dupen, D. W., 1966, *The Story of Stanford's Two-Mile-Long Accelerator*, SLAC-62, May. [SRDB Ref ID: 23307, p. 162]
- ERDA (Energy Research and Development Administration), 1975, "Chapter 0528, ERDA Contractor Occupational Medical Program Handbook," *ERDA Manual*, August 21. [SRDB Ref ID: 4643]
- ESHD (Environment, Safety and Health Division), 1992a, *Annual Environmental Monitoring Report, January – December, 1990*, SLAC-416, Stanford University, Stanford Linear Accelerator Center, Stanford, California. [SRDB Ref ID: 23204]
- ESHD (Environment, Safety and Health Division), 1992b, *Annual Environmental Monitoring Report, January – December, 1991*, SLAC-404, Stanford University, Stanford Linear Accelerator Center, Stanford, California. [SRDB Ref ID: 23207]
- ESHD (Environment, Safety and Health Division), 1993, *Annual Site Environmental Report, January – December, 1992*, SLAC-4425, Stanford University, Stanford Linear Accelerator Center, Stanford, California. [SRDB Ref ID: 23211]
- ESHD (Environment, Safety and Health Division), 1994, *1993 Site Environmental Report, January – December, 1993*, SLAC-440, Stanford University, Stanford Linear Accelerator Center, Stanford, California. [SRDB Ref ID: 23212]

- ESHD (Environment, Safety and Health Division), 1995, *1994 Site Environmental Report, January – December, 1994*, SLAC-R-95-468, Stanford University, Stanford Linear Accelerator Center, Stanford, California. [SRDB Ref ID: 23213]
- ESHD (Environment, Safety and Health Division), 1996, *1995 Site Environmental Report, January – December, 1995*, SLAC-R-486, Stanford University, Stanford Linear Accelerator Center, Stanford, California. [SRDB Ref ID: 23214]
- ESHD (Environment, Safety and Health Division), 1997, *1996 Site Environmental Report, January – December, 1996*, SLAC-R-507, Stanford University, Stanford Linear Accelerator Center, Stanford, California. [SRDB Ref ID: 23219]
- ESHD (Environment, Safety and Health Division), 1998a, *1997 Site Environmental Report, January – December, 1997*, SLAC-R-525, Stanford University, Stanford Linear Accelerator Center, Stanford, California. [SRDB Ref ID: 23220]
- ESHD (Environment, Safety and Health Division), 1998b, *Annual Site Environmental Report, January – December, 1998*, SLAC-R-535, Stanford University, Stanford Linear Accelerator Center, Stanford, California. [SRDB Ref ID: 23221]
- ESHD (Environment, Safety and Health Division), 2000, *Annual Site Environmental Report, January – December, 1999*, SLAC-R-555, Stanford University, Stanford Linear Accelerator Center, Stanford, California. [SRDB Ref ID: 23229]
- ESHD (Environment, Safety and Health Division), 2001, *Annual Site Environmental Report, January – December, 2000*, SLAC-R-572, Stanford University, Stanford Linear Accelerator Center, Stanford, California. [SRDB Ref ID: 23230]
- ESHD (Environment, Safety and Health Division), 2003, *Annual Site Environmental Report, January – December, 2001*, SLAC-R-601, Stanford University, Stanford Linear Accelerator Center, Stanford, California. [SRDB Ref ID: 23237]
- ESHD (Environment, Safety and Health Division), 2006a, *Annual Site Environmental Report: 2002*, SLAC-R-787, Stanford University, Stanford Linear Accelerator Center, Stanford, California. [SRDB Ref ID: 25392]
- ESHD (Environment, Safety and Health Division), 2006b, *Annual Site Environmental Report: 2003*, SLAC-R-788, Stanford University, Stanford Linear Accelerator Center, Stanford, California. [SRDB Ref ID: 25393]
- ESHD (Environment, Safety and Health Division), 2006c, *Annual Site Environmental Report: 2004*, SLAC-R-789, Stanford University, Stanford Linear Accelerator Center, Stanford, California. [SRDB Ref ID: 25395]
- ESO (Environment and Safety Office), 1986, *Annual Environmental Monitoring Report, January – December, 1985*, SLAC-295, Stanford University, Stanford Linear Accelerator Center, Stanford, California. [SRDB Ref ID: 23190]
- ESO (Environment and Safety Office), 1987, *Annual Environmental Monitoring Report, January – December, 1986*, SLAC-311, Stanford University, Stanford Linear Accelerator Center, Stanford, California. [SRDB Ref ID: 23193]

- ESO (Environment and Safety Office), 1988, *Annual Environmental Monitoring Report, January – December, 1987*, SLAC-326, Stanford University, Stanford Linear Accelerator Center, Stanford, California. [SRDB Ref ID: 23196]
- ESO (Environment and Safety Office), 1989, *Annual Environmental Monitoring Report, January – December, 1988*, SLAC-341, Stanford University, Stanford Linear Accelerator Center, Stanford, California. [SRDB Ref ID: 23200]
- ESO (Environment and Safety Office), 1990, *Annual Environmental Monitoring Report, January – December, 1989*, SLAC-363, Stanford University, Stanford Linear Accelerator Center, Stanford, California. [SRDB Ref ID: 23201]
- Flood, J. R., 1995a, "Panasonic UD-802 Lower Limit of Detection," memorandum to file, Stanford University, Stanford Linear Accelerator Center, Stanford, California, August 3. [SRDB Ref ID: 23307, p. 254]
- Flood, J. R., 1995b, "Dose Algorithm Reporting Criteria and Printouts", letter to D. Boling (ISA-The Dosimetry Management Company), Stanford University, Stanford Linear Accelerator Center, Stanford, California, May 5. [SRDB Ref ID: 23307, p. 337]
- Flood, J. R., 1995c, "Upper Useful Range of the Panasonic UD-802 Dosimeter", memorandum to files, Stanford University, Stanford Linear Accelerator Center, Stanford, California, September 6. [SRDB Ref ID: 25385]
- Flood, B., 1997, "Recalculation of Lower Limit of Detection for the Panasonic UD-802 Dosimeter", memorandum to files, Stanford University, Stanford Linear Accelerator Center, Stanford, California, June 24. [SRDB Ref ID: 26121]
- Flood, B., 2000a, "Revision of Background Subtraction Methodology", memorandum to file, Stanford University, Stanford Linear Accelerator Center, Stanford, California, July 20. [SRDB Ref ID: 25381]
- Flood, B., 2000b, "Revised Neutron Dose Conversion Factors for Personnel Dose Calculations", memorandum to file, Stanford University, Stanford Linear Accelerator Center, Stanford, California, March 1. [SRDB Ref ID: 25386]
- Freehafer, B., 1964, "Waiver of Physical Exams," memorandum to B. S. Kaiser with markups, Stanford University, Stanford Linear Accelerator Center, Stanford, California, May 6. [SRDB Ref ID: 23256, p 4]
- Frey, S. R., 2003, "ALARA Committee, Minutes of the meeting held March 11, 2003." [SRDB Ref ID: 23197]
- Gesell, T. F., 1986, DOELAP Performance Evaluation Program Administrator letter to D. Busick (Stanford Linear Accelerator Center), December 23. [SRDB Ref ID: 25384, p. 8]
- Gherman, M., 2006, collection of medical documents including "Consent for Medical Care," "Employee Information," "Initial Medical History," "Physical Examination Form," "Audiogram," "Physical Worksheet," "Letter to employee re Periodic Medical Exam," and list of procedures, Stanford University, Stanford Linear Accelerator Center, Stanford, California, April 11. [SRDB Ref ID: 23308]

- Gooch, A., 2005, completed "SLAC RP Radiological Air Sample Form," Stanford University, Stanford Linear Accelerator Center, Stanford, California, November 22. [SRDB Ref ID: 23198]
- Grissom, M. P., 1995, "ALARA Committee, Minutes of the meeting held April 27, 1995." [SRDB Ref ID: 23222]
- Grissom, M. P., 1997, "ALARA Committee, Minutes of the meeting held June 12, 1997." [SRDB Ref ID: 23231]
- HPS (Health Physics Staff), 1975, *Annual Environmental Monitoring Report, January – December, 1974*, SLAC-182, Stanford University, Stanford Linear Accelerator Center, Stanford, California. [SRDB Ref ID: 23158]
- HPS (Health Physics Staff), 1976, *Annual Environmental Monitoring Report, January – December, 1975*, SLAC-194, Stanford University, Stanford Linear Accelerator Center, Stanford, California. [SRDB Ref ID: 23170]
- HPS (Health Physics Staff), 1977, *Annual Environmental Monitoring Report, January – December, 1976*, SLAC-201, Stanford University, Stanford Linear Accelerator Center, Stanford, California. [SRDB Ref ID: 23171]
- HPS (Health Physics Staff), 1978, *Annual Environmental Monitoring Report, January – December, 1977*, SLAC-208, Stanford University, Stanford Linear Accelerator Center, Stanford, California. [SRDB Ref ID: 21899]
- HPS (Health Physics Staff), 1979, *Annual Environmental Monitoring Report, January – December, 1978*, SLAC-218, Stanford University, Stanford Linear Accelerator Center, Stanford, California. [SRDB Ref ID: 21900]
- HPS (Health Physics Staff), 1980, *Annual Environmental Monitoring Report, January – December, 1979*, SLAC-228, Stanford University, Stanford Linear Accelerator Center, Stanford, California. [SRDB Ref ID: 23172]
- ICRP (International Commission on Radiological Protection), 1979, *Limits for the Intake of Radionuclides by Workers, Part 1*, Publication 30, Part 1, Pergamon Press, Oxford, England.
- ICRP (International Commission on Radiological Protection), 1994, *Human Respiratory Tract Model for Radiological Protection*, Publication 66, Pergamon Press, Oxford, England.
- ICRP (International Commission on Radiological Protection), 1995, *Dose Coefficients for Intakes of Radionuclides by Workers*, Publication 68, Pergamon Press, Oxford, England.
- ICRP (International Commission on Radiological Protection), 1996, *Conversion Coefficients for Use in Radiological Protection Against External Radiation*, Publication 74, Pergamon Press, Oxford, England.
- ICRU (International Commission on Radiation Units and Measurements), 1992, *Measurement of Dose Equivalents from External Photon and Electron Radiations*, Report 47, Bethesda, Maryland.

- ICRU (International Commission on Radiation Units and Measurements), 1999, *Nuclear Data for Neutron and Proton Radiotherapy and for Radiation Protection*, Report 63, Bethesda, Maryland.
- Jenkins, T. M., 1964a, "Waiver of Physical Exams, etc.," memorandum to B. S. Kaiser, Stanford University, Stanford Linear Accelerator Center, Stanford, California, May 4. [SRDB Ref ID: 23256 pg 3, Freehafer]
- Jenkins, T. M., 1964b, "Film Badge Service; Reference Number 265, July 7, 1964," memorandum to D. Littlefield, Stanford University, Stanford Linear Accelerator Center, Stanford, California, July 29. [SRDB Ref ID: 23253]
- Jenkins, T. M., 1974, Accelerator Boundary Doses and Skyshine, *Health Physics*, volume 27, pp. 251–257. [SRDB Ref ID: 23176]
- Jenkins, T. M., 1979, "Neutron and Photon Measurements through Concrete from a 15 GeV Electron Beam on a Target – Comparison with Models and Calculations," *Nuclear Instruments and Methods in Physical Research*, Section A, volume 159, pp. 265–288. [SRDB Ref ID: 25399]
- Jenkins, T. M., and D. D. Busick, 1987, *Personnel Dose Equivalent Monitoring at SLAC Using Lithium-Fluoride TLDs*, SLAC TN 87-2, Stanford University, Stanford Linear Accelerator Center, Stanford, California, March. [SRDB Ref ID: 22849]
- Jenkins, T. M., R. C. McCall, and G. J. Warren, 1965, *Radiation Protection Problems at the Stanford Two Mile Linear Accelerator*, SLAC-PUB-151, November. [SRDB Ref ID: 23178]
- Kase, K. R., R. Sit, J. Liu, H. Tran, D. Busick, and M. Grissom, 1993, *Establishment of a Technical Basis for Internal Dosimetry at High Energy (50 GeV) Electron Accelerator Facilities*, SLACID001, July 14. [SRDB Ref ID: 23307, p. 497]
- Knoll, G. F. 1989, *Radiation Detection and Measurement*, Second Edition, John Wiley & Sons.
- Liu, J. C., D. Busick, K. R. Kase, R. C. McCall, R. Sit, and H. Tran, 1995, *Perspective of Personnel External Dosimetry at Stanford Linear Accelerator Center*, SLAC-PUB-95-6749, Stanford University, Stanford Linear Accelerator Center, Stanford, California, March. [SRDB Ref ID: 23307, p. 62]
- Liu, J. C., B. Flood, S. Rokni, R. Seefred, R. Sit, 2000, Use of LiF and Panasonic TLDs inside 5" and 6" Polyethylene Moderators for Area Dose Monitoring at SLAC, RP Note 99-14, Revision 1, Stanford University, Stanford Linear Accelerator Center, Stanford, California, March 21. [SRDB Ref ID: 23300]
- Liu, J. C., T. M. Jenkins, R. C. McCall, and N. E. Ipe, 1991, *Neutron Dosimetry at SLAC: Neutron Sources and Instrumentation*, SLAC-TN-91-3, Stanford University, Stanford Linear Accelerator Center, Stanford, California, October. [SRDB Ref ID: 23326]
- Liu, J. C., R. Seefred, and R. Sit, 1999, *Calibration Summary of Neutron Sources and Neutron Detectors*, SLAC RP 98-3 (March 1998) Revised, Stanford University, Stanford Linear Accelerator Center, Stanford, California, July. [SRDB Ref ID: 23301]

- Liu, J. C., A. Fasso, H. Khater, A. Prinz, and S. Rokni, 2004a, *Generic Radiation Safety Design for SSRL Synchrotron Radiation Beamlines*, RP-Note-03-21 Rev. 1, February 14. [SRDB Ref ID: 25405]
- Liu, J. C., A. Fasso, A. Prinz, and S. Rokni, 2004b, *Radiation Safety Design for SSRL Wiggler Beamline BL11*, RP Note 04-05 Rev.2, March 19. [SRDB Ref ID: 25409]
- Loesch, R. M., 2004, "Laboratory Accreditation of Stanford Linear Accelerator Center Personnel Dosimetry," memorandum to J. Muhlestein (Stanford Site Office), U.S. Department of Energy, Office of Quality Assurance Programs, Rockville, Maryland, December 20. [SRDB Ref ID: 23302]
- Margaritondo, G., 1988, *Introduction to Synchrotron Radiation*, Oxford University Press, New York, NY.
- McCall, R. C., 1968, *Use of Light Source for Testing Thermoluminescent Dosimeter Readers*, SLAC-PUB-459, July. [SRDB Ref ID: 23537]
- McCall, R. C., 1985, "Calibration of our $^{238}\text{PuLi}$ Source", memorandum to file, Stanford University, Stanford Linear Accelerator Center, Stanford, California, June 28. [SRDB Ref ID: 25396]
- McCall, R. C. 1988, "Neutron Source", memorandum to file, Stanford University, Stanford Linear Accelerator Center, Stanford, California, August 5. [SRDB Ref ID: 25400]
- McCall, R. C., 1991, *Beta-Ray Exposure from Work on Components with Induced Radioactivity from High-Energy Accelerators*, SLAC-TN-91-12, Stanford University, Stanford Linear Accelerator Center, Stanford, California, October. [SRDB Ref ID: 23307, p. 102]
- McCall, R. C., and T. M. Jenkins, 1966, *Preliminary Plan for Environmental Monitoring at SLAC*, TN-66-9, Stanford University, Stanford Linear Accelerator Center, Stanford, California, March. [SRDB Ref ID: 23245]
- MCC (Monsanto Chemical Company), 1977, Quotation 2/28 and attached documents on other sources. [SRDB Ref ID: 25401]
- Muhlestein, J. S., 2001, "Stanford Linear Accelerator Center (SLAC) Request for Approval of Internal Dosimetry Program," letter to K. R. Kase (Stanford Linear Accelerator Center), U.S. Department of Energy, Stanford Site Office, Stanford, California, February 23. [SRDB Ref ID: 23404]
- Nelson, W. R., 1987, *Properties of the E-M Cascade: A Tutorial Utilizing High Resolution 3D Color Graphics*, SLAC-PUB-4203, Stanford University, Stanford Linear Accelerator Center, Stanford, California, February 1987. [SRDB Ref ID: 23307, p. 140]
- NCRP (National Council on Radiation Protection and Measurements), 1971, *Protection Against Neutron Radiation*, Report 38, Bethesda, Maryland, January 4. [SRDB Ref ID: 11520]
- NCRP (National Council on Radiation Protection and Measurements), 1987, *Ionizing Radiation Exposure of the Population of the United States*, Report 93, Bethesda, Maryland, September 1.

- NCRP (National Council on Radiation Protection and Measurements), 2003, *Radiation Protection for Particle Accelerator Facilities*, Report 144, Bethesda, Maryland, December.
- NIOSH (National Institute for Occupational Safety and Health), 2002, *External Dose Reconstruction Implementation Guideline*, OCAS-IG-001, Rev. 1, Office of Compensation Analysis and Support, Cincinnati, Ohio, August.
- Operational Health Physics (OHP) Staff and Plant Engineering Department, 1985, *Annual Environmental Monitoring Report, January – December, 1984*, SLAC-280, Stanford University, Stanford Linear Accelerator Center, Stanford, California. [SRDB Ref ID: 23188]
- Oak Ridge Associated Universities Team (ORAUT) *Technical Basis for Conversion from NCRP Report 38 Neutron Quality Factors to ICRP Publication 60 Radiation Weighting Factors for Respective IREP Input Neutron Energy Ranges*, June, 2006, ORAUT-OTIB-0055.
- Piesch, E., and B. Burgkhardt, 1978, "The Role of an Analyzer Type Albedo Dosimeter in Routine Monitoring and the Current Situation for the Calibration Technique," *Seventh DOE Workshop on Personnel Neutron Dosimetry*, PNL-2807, Pacific Northwest Laboratory, Richland, Washington. [SRDB Ref ID: 26723]
- Pindar, F. V. L., 1965a, "Medical Exams – 6/1/65 revision of University Administrative Guide Memo 22.1.5.c.," memorandum to Moulton et al., June 28. [SRDB Ref ID: 23215]
- Pindar, F., 1965b, "Blanket Order, Palo Alto Medical Clinic, Req. 24789M," memorandum to D. Littlefield, Stanford University, Stanford Linear Accelerator Center, Stanford, California, June 29. [SRDB Ref ID: 23251]
- Radcal, 1991, *Certificate of Conformance*, October 24. [SRDB Ref ID: 25383]
- RPHP (Radiation Physics Staff and Health Physics Staff), 1981, *Annual Environmental Monitoring Report, January – December, 1980*, SLAC-242, Stanford University, Stanford Linear Accelerator Center, Stanford, California. [SRDB Ref ID: 23177]
- RPHP (Radiation Physics Staff and Health Physics Staff), 1982, *Annual Environmental Monitoring Report, January – December, 1981*, SLAC-249, Stanford University, Stanford Linear Accelerator Center, Stanford, California. [SRDB Ref ID: 23186]
- RPHP (Radiation Physics Staff and Health Physics Staff), 1983, *Annual Environmental Monitoring Report, January – December, 1982*, SLAC-260, Stanford University, Stanford Linear Accelerator Center, Stanford, California. [SRDB Ref ID: 23187]
- RPHP (Radiation Physics Staff and Health Physics Staff), 1984, *Annual Environmental Monitoring Report, January – December, 1983*, SLAC-271, Stanford University, Stanford Linear Accelerator Center, Stanford, California. [SRDB Ref ID: 23188]
- Rickansrud, E. B., 1968, "AEC Required Reports", memorandum to R. C. McCall. [SRDB Ref ID: 23238]
- Rickansrud, E. B. 1986, "Application for Accreditation in Personnel Dosimetry", letter to J. T. Davis (U.S. Department of Energy, San Francisco Operations Office), March 24. [SRDB Ref ID: 25382]

Rohrig, N. 2006a, CAP-88 Calculation.

Rohrig, N. 2006b, EXCEL Spreadsheet, *SLAC Science*.

Rokni, S. H., T. Gwise, J. C. Liu, S. Roesler, and A. Fasso, 2001, *Induced Radioactivity of Materials by Stray Radiation Fields at an Electron Accelerator*, SLAC-PUB-8912, Stanford University, Stanford Linear Accelerator Center, Stanford, California, July. [SRDB Ref ID: 23429]

Sit, R., 1995, "Lower Limit of Detectability of LiF TLDs," memorandum to file, Stanford University, Stanford Linear Accelerator Center, Stanford, California, July 7. [SRDB Ref ID: 23307, p. 423]

Sit, R., 2000, *OHP Department Airborne Activity Control Levels*, SLAC-I-760-2A05O-009, FO# 012, Rev. 6, Stanford University, Stanford Linear Accelerator Center, Stanford, California, October 5. [SRDB Ref ID: 23364]

Stanford University, 2005, *Radiologically Controlled Areas*, Drawing 8473A3, Stanford Linear Accelerator Center, Stanford, California, May. [SRDB Ref ID: 23381]

Stanford University, 2006, *SPEAR 3 Final Safety Assessment Document*, Rev. 1, Stanford, California, February. [SRDB Ref ID: 26122]

Svensson, G. K., R. C. McCall, and G. L. Babcock, 1970, *An Improved TLD Reader*, SLAC-PUB-731, Stanford University, Stanford Linear Accelerator Center, Stanford, California, April. [SRDB Ref ID: 23517]

Taniguchi, S., T. Nakamura, T. Nunomiya, H. Iwase, S. Yonai, M. Sasaki, S. H. Rokni, J. C. Liu, K. R. Kase, and S. Roesler, 2003, "Neutron Energy and Time-of-Flight Spectra behind the Lateral Shield of a High Energy Electron Accelerator Beam Dump, Part I: Measurements," *Nuclear Instruments and Methods in Physical Research*, Section A, volume 503, pp. 595–605. [SRDB Ref ID: 23305]

Tran, H., 2004a, *SLAC External Dosimetry Program Manual*, SLAC-I-760-2A07F-001-Rev. 2, DG #101, Rev. 2, Stanford University, Stanford Linear Accelerator Center, Stanford, California, August 17. [SRDB Ref ID: 23314]

Tran, H., 2004b, *Dose Processing and Reporting Procedure*, SLAC-I-760-2A07H-001-R2.0, DG #004, Rev. 2.0, Stanford University, Stanford Linear Accelerator Center, Stanford, California, August 17. [SRDB Ref ID: 23112]

Tran, H., 2005, *Technical Basis Regarding Routine Bioassay Measurements at SLAC*, DG #103, Rev. 3.0, Stanford University, Stanford Linear Accelerator Center, Stanford, California, April 15. [SRDB Ref ID: 23355]

Tran, H., 2006, "Responses to SLAC Questions," Stanford University, Stanford Linear Accelerator Center, Stanford, California, June 30. [SRDB Ref ID: 25410]

UNSCEAR (United Nations Scientific Committee on the Effects of Atomic Radiation), 1988, *Sources and Effects of Ionizing Radiation*, with Annexes, United Nations, New York, New York. Available on-line at <http://www.unscear.org/unscear/en/publications.html>

Vylet, V, J. C. Liu, S. H. Rokni, and L. -X. Thai, 1997, "Measurements of Neutron Spectra at the Stanford Linear Accelerator Center," *Radiation Protection Dosimetry*, volume 70, pp. 425–428. [SRDB Ref ID: 23306]

Vylet, V and J. C. Liu, 2002, *Radiation Protection at High-Energy Electron Accelerators*, SLAC-PUB-9557, October. [SRDB Ref ID: 23412]

Wiedemann, H. 1998, *Synchrotron Radiation Primer*, October. [SRDB Ref ID: 25413]

GLOSSARY

absorption

Process in which energy of radiation is transferred to the material it traverses.

accelerator

See *particle accelerator*.

activation

The process of inducing radioactivity by irradiation.

annihilation

A process in which a particle meets its corresponding antiparticle and both disappear. Their energy and momentum appear in some other form, producing other particles together with their antiparticles and providing their motion.

antiparticle

In particle physics every particle with any type of charge or fermion label has a corresponding antiparticle type. Any particle and its antiparticle have identical mass and spin but opposite charges. For example, the antiparticle of an electron is a positron. It has exactly the same mass as an electron but a positive charge.

attenuation

Process by which absorption and scattering reduces the number of particles or photons entering a body of matter.

BaBar

Official name for SLAC B Factory detector. Also known as B B-bar detector. Named after the elephant in Laurent DeBrunhoff's children's books, with permission of DeBrunhoff's estate.

becquerel

International System unit of radioactivity equal to 1 disintegration per second; 1 curie equals 37 billion (3.7×10^{10}) Bq.

beta radiation

Charged particle emitted from some radioactive elements with a mass equal to 1/1,837 that of a proton. A negatively charged beta particle is identical to an electron. A positively charged beta particle is a positron. Most of the direct fission products are (negative) beta emitters. Exposure to large amounts of beta radiation from external sources can cause skin burns (erythema), and beta emitters can be harmful inside the body. Thin sheets of metal or plastic can stop beta particles.

Beam Switch Yard (BSY)

The end of the LINAC where beams are switched to the SLC arcs, the PEP ring, the SLC, or end station areas A, B, or C.

B Factory

One of two high-energy physics facilities currently in operation in the United States (SLAC) and Japan (KEK). Both B Factories collide electrons with positrons to produce large numbers of B mesons (bound states of a bottom quark and an antidown quark) and anti-B mesons. By measuring the difference in decays of B and anti-B mesons, physicists hope to understand CP

violation, thought to be the reason why matter dominates in the universe. At SLAC, the B Factory accelerates electrons at 9 GeV and positrons at 3.1 GeV.

claimant

Individual who has filed for compensation under the Energy Employees Occupational Illness Compensation Program.

contamination

Radioactive material in an undesired location including air, soil, buildings, animals, and persons.

Columbia Resin 39 (CR-39)

Material (allyl diglycol carbonate) used for detecting neutrons. Radiation damage from recoiling protons is etched away allowing visualization of damage and estimation of neutron dose. Also used for face shields on motorcycle helmets.

curie (Ci)

Traditional unit of radioactivity equal to 37 billion (3.7×10^{10}) becquerels (Bq), which is approximately equal to the activity of 1 gram of pure ^{226}Ra .

dosimeter

Device that measures the quantity of received radiation, usually a holder with radiation-absorbing filters and radiation-sensitive inserts packaged to provide a record of absorbed dose received by an individual.

dosimetry

Measurement and calculation of internal and external radiation doses.

electron

Basic atomic particle with negative charge and a mass 1/1,837 that of a proton. Electrons surround the positively charged nucleus of the atom.

gamma ray, particle, or photon

See *gamma radiation*.

gamma radiation

Electromagnetic radiation (photons) of short wavelength and high energy (10 kiloelectron-volts to 9 megaelectron-volts) that originates in atomic nuclei and accompanies many nuclear reactions (e.g., fission, radioactive decay, and neutron capture). Gamma rays are very penetrating, but dense materials such as lead or uranium or thick structures can stop them. Gamma photons are identical to X-ray photons of high energy; the difference is that X-rays do not originate in the nucleus.

half-life

Time in which half of a given quantity of a particular radionuclide disintegrates (decays) into another nuclear form. During one half-life, the number of atoms of a particular radionuclide decreases by one half. Each radionuclide has a unique half-life ranging from millionths of a second to billions of years.

high-energy physics

A branch of science that tries to understand the interactions of the fundamental particles such as electrons, photons, neutrons and protons (and many others that can be created). This type of physics is called *high-energy* because very powerful machines, such as the Two-Mile Accelerator at SLAC, are created to make these particles go very fast so they can probe deeply into other particles and try to understand what they are made of.

ionizing radiation

Radiation of high enough energy to remove an electron from a struck atom and leave behind a positively charged ion. High enough doses of ionizing radiation can cause cellular damage. Ionizing particles include alpha particles, beta particles, gamma rays, X-rays, neutrons, high-speed electrons, high-speed protons, photoelectrons, Compton electrons, positron/negatron pairs from photon radiation, and scattered nuclei from fast neutrons. See *beta radiation*, *gamma radiation*, *neutron radiation*, *photon radiation*, and *X-ray radiation*.

isotope

One of two or more atoms of a particular element that have the same number of protons (atomic number) but different numbers of neutrons in their nuclei (e.g., ^{234}U , ^{235}U , and ^{238}U). Isotopes have very nearly the same chemical properties but often have different physical properties.

klystron

Evacuated electron tube used as an oscillator or amplifier at microwave frequencies. In the klystron, an electron beam is velocity-modulated (periodically bunched) to produce large amounts of power. A klystron can be a source of X-rays.

linear accelerator (LINAC)

Straight single-pass particle accelerator in which radio frequencies accelerate the beam over the length of the accelerator. The SLAC LINAC is a 2-mi-long accelerator, consisting of a cylindrical, disc-loaded, copper waveguide placed on concrete girders in a tunnel about 25 ft underground.

micro-

Prefix that divides a unit by 1 million (multiplies by 1×10^{-6}).

milli-

Prefix that divides a unit by 1,000 (multiplies by 1×10^{-3}).

nano-

Prefix that divides a unit by 1 billion (multiplies by 1×10^{-9}).

neutron

Basic nucleic particle that is electrically neutral with mass slightly greater than that of a proton. There are neutrons in the nuclei of every atom heavier than normal hydrogen.

neutron radiation

Radiation that consists of free neutrons unattached to other subatomic particles. Neutron radiation can cause further fission in fissionable material such as the chain reactions in nuclear reactors, and nonradioactive nuclides can become radioactive by reactions creating neutrons or by absorbing free neutrons. See *neutron*.

nucleus

Central core of an atom, which consists of positively charged protons and, with the exception of ordinary hydrogen, electrically neutral neutrons. The number of protons (atomic number) uniquely defines a chemical element, and the number of protons and neutrons is the mass number of a nuclide. The plural is nuclei.

nuclide

Stable or unstable isotope of any element. Nuclide relates to the atomic mass, which is the sum of the number of protons and neutrons in the nucleus of an atom. A radionuclide is an unstable nuclide.

photopion production

Reaction where a high-energy photon interacts with a nucleus and emits a pi meson and a high-energy neutron.

pair production and annihilation

Production of a particle and its matching antiparticle whenever sufficient energy is available to provide the mass-energy. When a particle collides with its matching antiparticle they could annihilate – which means they both disappear and their energy appears as some other particles – with a balanced number of particles and antiparticles for each type. All conservation laws are obeyed in these processes.

particle accelerator

Device that accelerates (imparts energy to) ions using magnetic or electrostatic fields and radiofrequency fields for focusing and redirecting ion beams. The main purposes of accelerators are the investigation of high-energy particle behavior and synthetic isotopes. The accelerator at SLAC is an electron accelerator.

photon

Basic unit of electromagnetic radiation. Photons are massless “packages” of light energy that range from low-energy microwave photons and visible light to high-energy gamma rays. Photons have energies between 1 nanoelectron-volt and 1000 gigaelectron-volt. See *photon radiation*.

photon radiation

Electromagnetic radiation of light energy (photons) from microwaves to gamma rays. Gamma rays and X-rays are examples of ionizing photon radiation, which have enough energy to penetrate matter, including the body, and deposit energy in that matter.

positron

Subatomic particle identical to an electron but with a positive charge; antiparticle of the electron. See *electron*.

proton

Basic nucleic particle with a positive electrical charge and mass slightly less than that of a neutron. There are protons in the nuclei of every atom, and the number of protons is the atomic number, which determines the chemical element.

quality factor

Historical value assigned to reflect the average effectiveness of a particular kind of radiation in producing biological effects in humans, now called radiation weighting factor. The quality

factor multiplied by the absorbed dose yields the dose equivalent. See *dose, relative biological effectiveness*, and *weighting factor*.

radiation

Subatomic particles and electromagnetic rays (photons) that travel from one point to another, some of which can pass through or partly through solid materials including the human body. See *ionizing radiation*.

radiation length

distance for the mean particle energy to decrease by a factor of 1/e, about 6 mm in lead and 20 cm in concrete

radioactive

Giving off ionizing radiation such as alpha particles or X-rays.

radioactivity

Disintegration of certain elements (e.g., radium, actinium, uranium, and thorium) accompanied by the emission of alpha, beta, gamma, and/or neutron radiation from unstable nuclei. See *radionuclide*.

radionuclide

Radioactive nuclide. See *radioactive* and *nuclide*.

rem

Traditional unit of radiation dose equivalent that indicates the biological damage caused by radiation equivalent to that caused by 1 rad of high-penetration X-rays multiplied by a quality factor. The average American receives 360 millirem a year from background radiation. The sievert is the International System unit; 1 rem equals 0.01 sievert. The word derives from roentgen equivalent in man; rem is also the plural.

shielding

Material or obstruction that absorbs ionizing radiation and tends to protect personnel or materials from its effects.

shower (also called electromagnetic cascade shower)

Electrons can create photons by interacting with a medium. In a similar way, photons can create electrons and their antiparticles, positrons, by interacting with a medium. So, imagine a very high-energy electron, of the sort used at SLAC, impinging on some material. The electron can set photons into motion and these photons can, in turn, set electrons and positrons into motion, and this process can continue to repeat. One high-energy electron can set thousands of particles into motion. Albert Einstein's famous relation governing the equivalence of matter and energy ($E = mc^2$) governs this process—namely, that matter (electrons and positrons) can be created from pure energy and vice versa. The particle creation process only stops when the energy runs out.

storage ring

A circular (or near circular) structure in which either high-energy electrons and/or positrons, or protons and/or antiprotons can be circulated many times and thus "stored." Used to achieve high-energy collisions. Because of the very different masses of protons and electrons, a storage ring design must accommodate one or the other type and cannot work for both.

synchrotron

Roughly circular particle accelerator in which the particles travel in synchronized bunches at fixed radius.

synchrotron radiation

Radiation emitted by charged particles traveling in the arc of a circle, which is undergoing acceleration due to its change in direction. When a charged particle undergoes accelerated motion it radiates electromagnetic energy. A common example is the emission of radio waves when electrons move back and forth in a radio antenna. This radiation is particularly intense and very directional when electrons traveling at close to the speed of light are bent in magnetic fields.

X-ray radiation

Penetrating electromagnetic radiation (photons) of short wavelength (0.001 to 10 nanometers) and energy less than 250 kiloelectron-volts. X-rays usually come from excitation of the electron field around certain nuclei but can also come from synchrotron radiation and bremsstrahlung. Once formed, there is no difference between X-rays and gamma rays, but gamma photons originate inside the nucleus of an atom.

ATTACHMENT A
HIGH ENERGY TLD NEUTRON DOSIMETRY
Page 1 of 10

The neutron energy spectra at SLAC shown in Figures 2-3 to 2-6 presumably extend almost from the beam energy, several GeV, down to thermal energies at 10^{-2} eV. In practice, the neutron energies extend only up to somewhat above 200 MeV, so the neutron energies only cover 10 orders of magnitude. The response of a system—whether it is an electronic instrument, a passive detector, a personnel dosimeter, or the biological effect in some tissue—to the neutrons can only be characterized as an integral of the product of the particular energy response function and the fluence as a function of energy over the energy range. Because of the wide neutron energy spectrum at SLAC, these responses are somewhat unusual. To measure the fluence as a function of energy requires a set of multiple detectors with responses that span the energy range and whose sensitivities are somewhat orthogonal, so the energy dependence of fluence can be estimated. An ideal dosimeter, which does not exist, has a response function that is a multiple of the response function for dose equivalent over the entire range of the neutron spectrum in the radiation field; alternatively stated, the response per unit dose equivalent should be independent of energy over the important energy range.

A comparison to gamma dosimetry is useful. The principal interaction for gamma radiation from 100 keV to 5 MeV is with electrons. Because electrons are all the same, the Bragg-Gray theorem implies that any device that measures energy deposition is a good dosimeter. For lower and higher energies, the Z enters the cross section, so all one needs to do is have low- Z material (hydrogen, carbon, nitrogen, and oxygen in about the same ratio as tissue) and one has a good dosimeter. Very high-energy photons are not an issue for dosimetry because there needs to be enough shielding for worker protection to eliminate them.

For neutrons, the energy is deposited in tissue primarily by proton recoil, so the energy dependences of the NTA and Neutrak 144 systems that use that process follow somewhat the energy dependence of the dose response. The Neutrak system becomes sensitive at about 20 to 50 keV, and the NTA becomes sensitive at about 800 keV; neutrons below those energies are not detected. These fractions are indicated in Table 6-5 for the spectral measurements discussed in Section 2.3.4.

Above 10 to 50 MeV, carbon and oxygen recoil and spallation become important. The NTA and Neutrak systems probably do not respond to them. There are no calibration sources in this energy range, so testing cannot occur. Based on ICRU Report 63 (1999, Figure 7.19) an estimated 30% to 40% of the dose equivalent in this energy range is lost.

In contrast to photons (where the photoelectric effect absorbs low-energy photons), for neutrons there are no big absorption processes in the 10-eV to 100-keV energy range, so lower energy neutrons must be considered. For neutron energies below 10 keV, neutrons scatter in the body until they reach thermal energies ($1/40$ eV) when the $1/v$ cross sections become important and they are absorbed by hydrogen (generates 2.2 MeV photon) or ^{14}N (yields ^{14}C and energetic proton recoil), which results in a nearly energy-independent dose conversion factor below 10 keV. Above 10 keV, the dose conversion factor is an increasing function of energy, and at 1 MeV it is a factor of 40 larger than below 10 keV. The proton recoil dose (10 keV to a few MeV) causes a surface dose that moves inward as the energy increases, but the thermal dose is a whole-body dose due to the weak attenuation of the 2.2-MeV photons. For high-energy neutrons, the maximum dose is deep in the body. For simplicity, all neutron dose equivalent has been historically treated as a whole-body dose.

ATTACHMENT A
HIGH ENERGY TLD NEUTRON DOSIMETRY
Page 2 of 10

SLAC had a fairly extensive system of neutron measurements, but they generally did not measure the complete neutron dose equivalent because it is extremely difficult to measure. Most neutron detection systems use a $1/v$ cross section in ${}^6\text{Li}(n,t)\alpha$ and ${}^{10}\text{B}(n,\alpha){}^7\text{Li}$ to measure low-energy neutrons. Figure A-1 from Knoll (1989, Figure 14-1) shows the cross sections used for monitoring slow neutrons in ${}^6\text{Li}$ (TLDs), ${}^{10}\text{B}$ (PMS, TLD), and ${}^3\text{He}$. Because these cross sections all have the same shape, calculations for one reaction like Figure A-2 can be applied to another reaction like TLDs in a moderator of similar thickness.

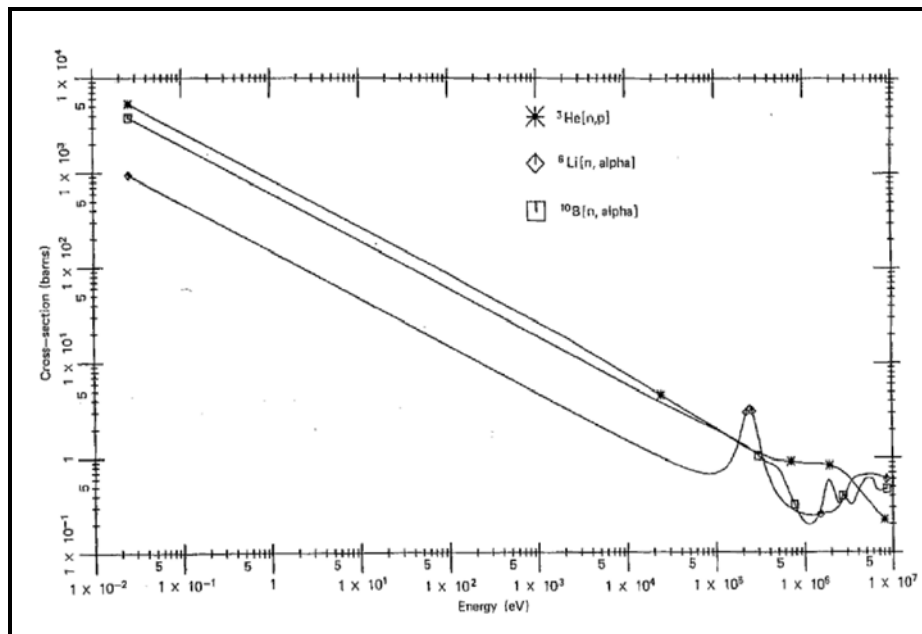


Figure A-1. Cross section versus neutron energy for some reactions of interest in neutron detection (Knoll 1989, Figure 14-1)

PMS Detectors

The moderated BF_3 counters used in the PMS use 2-in.-diameter BF_3 proportional counters surrounded with 6 cm of polyethylene in a cadmium can. The moderator changes the energy response of the thermal neutron detector into essentially a fluence detector in the energy range up to a few MeV. Figure A-2 shows the fluence response of this detector (Liu et al. 1991). The right-hand panel shows a digitization of the side incidence curve on the left-hand panel and the associated response per unit dose equivalent.

The triangles are responses to the four (α, n) calibration sources plotted at their average energies and are presumably high because of low-energy neutrons in the spectra where the instrument responds well. Because of the wide range of neutron energies and the large range of instrument sensitivity, the average energy is a nearly useless concept.

An ideal detector would have a uniform response per unit dose equivalent over the important energy range. In terms of dose equivalent, this detector under-responds to neutrons above about 10 keV and essentially responds only to neutrons below about 0.1 MeV. In the spectra of Figures 2-3 to 2-6 dose equivalent is important primarily in the range of 0.1 to 200 MeV. Figure A-3 shows the PMS response

**ATTACHMENT A
HIGH ENERGY TLD NEUTRON DOSIMETRY
Page 3 of 10**

along with the SLAC- and CERN-measured spectra. The fact that the response and the neutron dose are in different energy regions severely compromises the usefulness of the PMS system.

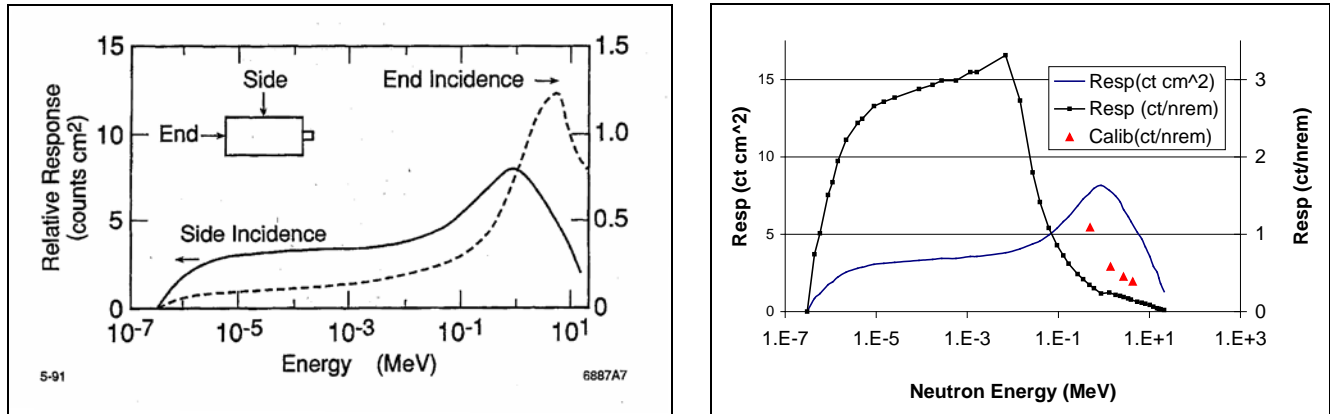


Figure A-2. Fluence and dose response vs. energy for PMS neutron detector (Liu et al. 1991) [11]

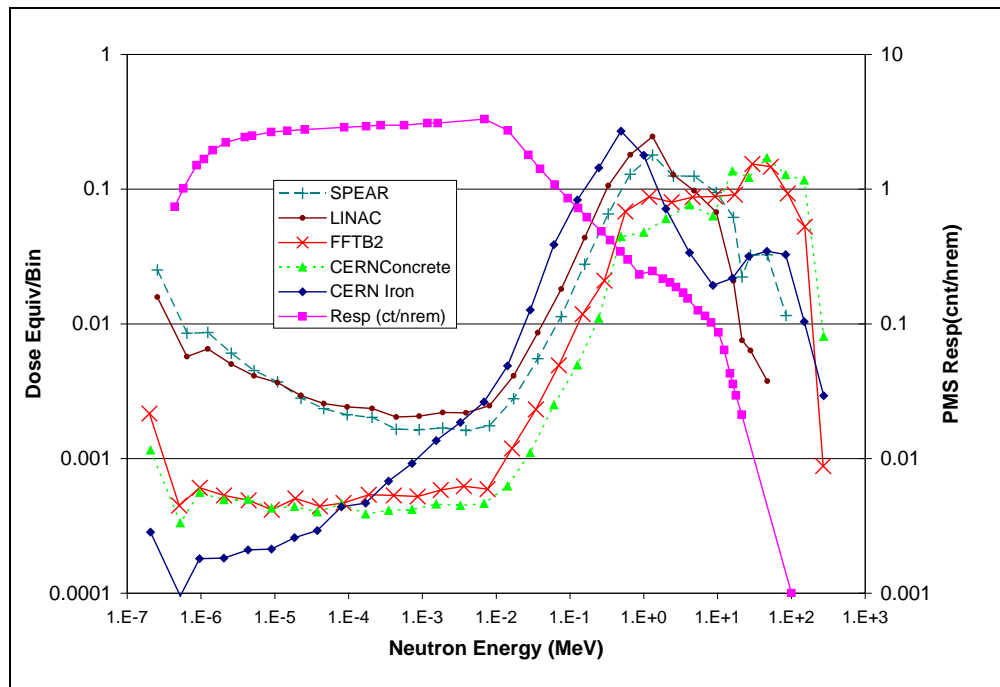


Figure A-3. Log plot of dose equivalent/bin for high-energy neutron spectra and PMS instrument response [12].

SLAC used moderated and bare BF₃ counters that would measure fast and thermal neutrons at several locations around the research area. The moderated counters had 6 cm of polyethylene surrounded by cadmium to absorb thermal neutrons; they would essentially measure the neutron flux from 0.4 eV to 5 MeV (see Figure A-2) called the moderated flux. TLDs in 6-in.-diameter cylindrical moderators in a cadmium can were used to monitor radiation fields at several places throughout the facility. These detectors have an energy response similar to that of the BF₃ PMS counters.

ATTACHMENT A
HIGH ENERGY TLD NEUTRON DOSIMETRY
Page 4 of 10

In the field, dose determination is more difficult because the neutron spectra extend to much higher energies than the calibration sources and most instruments. There are several measurements used to qualify the 5- and 6-in. moderated TLDs as a measurement tool (Liu et al. 2000). These instruments are characterized as providing information on the neutrons only below 20 MeV. Neutrons above 20 MeV are characterized as having up to as much dose in the SLAC radiation fields as the lower energy neutrons. For the SLAC radiation fields, the spectrum as well as the dose equivalent have not been readily available, so generating useful information for calibration has been very difficult.

The exceptions are the CERN high-energy calibrations. To reduce the lack of an adequate calibration source, the world's high-energy physicists have collaborated in an intercomparison program using the CERN CEC high-energy reference field facility. In these experiments, 205-GeV/c (250 GeV) protons struck a 50-cm-long copper target. Fields were measured at a 90° angle above a 40-cm-thick iron shield and above an 80-cm-thick concrete shield. Field standardization was provided by a tissue-equivalent proportional counter (TEPC) measurement and by cascade calculations using the FLUKA (FLUKtuierende Kaskade) software. The dose measurement with the TEPC starts near 50 keV neutron energy (below that is treated as gamma), so the TEPC yields a smaller dose than the FLUKA calculation and is not used here. For the CERN concrete spectrum, the fraction of low energy neutrons is much smaller, so the difference is not important. Spectra were measured with Bonner spheres, and the 6-in. TLD system was irradiated. One can integrate the product of the neutron dose spectra shown in Figure A-3 with the instrument response and calculate dose conversion factors for the PMS measurement device in the particular spectrum as shown in Table A-1. To integrate, the high-energy BF₃ instrument response is extrapolated above 18 MeV to 0.001 ct/nrem at 100 MeV and to zero at 1,000 MeV. Instrument response is interpolated to the geometric mean neutron energy in each spectrum bin.

Assuming that the PMS system and the 6-in.-diameter TLD system have the same energy response as shown in Figure A-2 and Figure A-3 on a logarithmic scale, one can compare the calculations to the measurement. For the CERN measurements with 6-in. moderated TLDs, the ratio of responses to the iron and concrete spectra was 5.5 (10/1.8). The ratio for the calculation was 4.0 (0.40/0.099), which demonstrated that the process was fairly well understood. The lack of complete agreement could be due to 1) differences between the reported spectra and reality, 2) differences in energy responses of the PMS moderated BF₃ detector and the 6-in. moderated TLD, or 3) errors in digitizing the various data. The first factor is considered most important. Note that the Figure A-3 spectra shape for the iron departs from all the other spectral shapes in the 1-eV region. The third factor could also be quite important in the 10-keV region where all the curves are changing rapidly.

SLAC used an Anderson-Braun neutron detector to provide measurement of a dose equivalent response up to about 20 MeV neutron energy. They also used a 9-in.-diameter Eberline sphere to measure dose equivalent in the same energy range. Like most accelerator laboratories, to measure neutrons above 20 MeV they would irradiate 5- by 5-in. plastic scintillators and then take them to a counter and count the ¹¹C decays in the plastic. The LINUS detector developed in 1990 uses a 1-cm-thick layer of lead in a moderator to provide a nearly dose equivalent measurement to high energies (Vylet et al. 1997).

Table A-1 also shows calculated H₂₆ values, which are the fractions of the dose above 26 MeV that varies from zero for the calibration sources (and thus their limited usefulness) to 40% for FFTB2 and 55% for the CERN concrete spectrum. Dose equivalent measurements are provided for the FFTB2 spectrum with the LINUS, which is assumed to measure the entire spectrum, and the Anderson-

ATTACHMENT A
HIGH ENERGY TLD NEUTRON DOSIMETRY
Page 5 of 10

Table A-1. Measured and calculated response.

Radiation field		CERN iron		CERN concrete		SSRL	SSRL	FFTB2		PuBe	PuB	PuF	PuLi	
Measurement	Units	<20 MeV	All	<20 MeV	All	LINAC	SPEAR		Ref.					Ref*
E_{av}	MeV					0.9	2.0	19.3	(a)	4.3	2.7	1.4	0.5	(b)
H_{26}	%		11.2		54.5	1.0	5.7	38.9	(a)	0	0	0	0	(b)
h_{phi}	nrem cm ²					8.5	7.4	24.	(a)					
h_{phi}	nrem cm ²		14.9 ^c		34.7 ^c	10.4	10.2	29.5	NRCalc ^d					
AndBraun	mrem/hr							13.3	(a)					
Linus	mrem/hr							22.0	(a)					
Bonner Sphere	mrem/hr					8.8	18.9	18.8	(a)					
PMS ModBF ₃	ct/nrem									0.389	0.451	0.582	1.09	(b)
PMS ModBF ₃	ct cm ²									14.7	16.9	18.8	18.3	(b)
TLD 6 in.	V/rem	11.4	10	3.6	1.8				(e)	1.94	1.91	3.21	5.49	(f)
C PMS Resp	ct/nrem		0.40		0.099	0.385	0.318	0.135	NRCalc					
LiF TLD	V/rem		5.90		3.90	38.4	51.9	5.45	NRCalc	0.45	0.394	0.814	1.45	(f)
Hankins TLD	R/rem		0.985		0.236	1.52	1.46	0.299	NRCalc					

a. Vylet et al. (1997).

b. Liu, Seefred, and Sit (1999).

c. These are the dose fractions above 20.5 MeV, not 26 MeV.

d. NRCalc Spreadsheet calculations based on folding measured spectra with calculated instrument responses and dose conversions as discussed in text (Rohrig 2006b).

e. Liu et al. (2000).

f. Liu et al. (1991).

ATTACHMENT A
HIGH ENERGY TLD NEUTRON DOSIMETRY
Page 6 of 10

Braun, which does a good job to about 10 MeV. The calculated dose equivalent rate from the Bonner sphere unfolding is considerably larger than the Anderson-Braun result, but not quite as large as the LINUS. The mean energies for the four (α, n) neutron sources are provided along with responses for the LiF TLD, 6-in. moderated TLD, and the PMS detectors. All responses increase with decreasing energy, and the PMS response is only about 1/10 the peak response at lower energies but significantly larger than the response at the mean energy, which demonstrates that the main signal is from neutrons where the spectrum is uncertain.

Based on Table A-1, the environmental neutron results in Tables 4-3 and 4-4 need to be adjusted. This analysis assumed that the reported PMS doses were based on PuF calibrations and will result in the largest adjusted doses for the sources SLAC had in the 1970s. Further, the analysis assumed that the skyshine neutron spectrum received by the detector or a casual visitor is best described by the SSRL LINAC spectrum. The correction is then $0.582 \div 0.385 = 1.51$ with an uncertainty of 35% at 1 sigma based on the ratio 5.5/4.1 from the measured to calculated ratios for moderated TLDs for the CERN iron and concrete spectra. If the FFTB2 was appropriate, the doses received would be smaller by about a factor of 3 ($0.385/0.135$) [13].

Albedo TLD Systems

In a similar fashion as the PMS system, one can consider the TLDs used for personnel monitoring. Albedo TLD neutron systems use a $1/v$ cross section in ${}^6\text{Li}(n,t)\alpha$ and ${}^{10}\text{B}(n,\alpha){}^7\text{Li}$ to measure low-energy neutrons leaving the body. Scattered neutrons from the body generate low-energy neutrons, which gives sensitivity to higher energy neutrons. The LiF and Panasonic systems used at SLAC use the albedo technique, but they do not follow the classic technique of using a cadmium case to absorb thermal neutrons, so these SLAC dosimeters over-respond to thermal neutrons. Figure A-4 shows the flux of neutrons below the cadmium cutoff (0.4 eV) and the next two higher energy groups leaving the body, which are detected with albedo systems as calculated by Alsmiller and Barish (1974, Figure 2) using discrete ordinates methods for monoenergetic neutrons up to 400 MeV. The SLAC systems detect all three groups shown in Figure A-3, whereas most albedo TLD systems only detect the two higher energy groups. At SLAC, the TLD reader gain is standardized with a particular ${}^{14}\text{C}$ source, so 1 mrem of ${}^{137}\text{Cs}$ gives light measured as 1 nC or 1 mV at the output of the light detector. For neutrons, SLAC uses a conversion factor of 1 mrem/nC or 1 mrem/mV of light output for the ${}^6\text{LiF}$ TLD dosimeters.

Figure A-5 (Piesch and Burgkhardt 1978) shows the neutron energy dependence of albedo systems up to 20 MeV but not to the 500 MeV available in SLAC neutrons. The response in Figure A-5 is an integral of the product of the cross section in Figure A-1 and the fluence in Figure A-4 divided by the flux-to-dose conversion factor. The primary cause of the factor of 1,000 response change from 10 eV to 10 MeV in Figure A-5 is the change in the flux-to-dose conversion factor just as it was in Figure A-2. Using the classic albedo system, a spectrum conversion factor can be estimated using the ratio of two measurements, but this was not done at SLAC. The effect of not having the cadmium covers is that the response of these SLAC dosimeters does not drop by 1 or 2 orders of magnitude for thermal neutrons as shown in Figure A-5 for other albedo dosimeters. In addition, the signal is higher because all three groups shown in Figure A-4 are measured. The cadmium cover eliminates the largest group.

To estimate the response of the SLAC LiF TLD system to all neutrons, this analysis considered how the TLD responds to the incoming radiation. A regular TLD signal is the integral of the product of the

ATTACHMENT A
HIGH ENERGY TLD NEUTRON DOSIMETRY
 Page 7 of 10

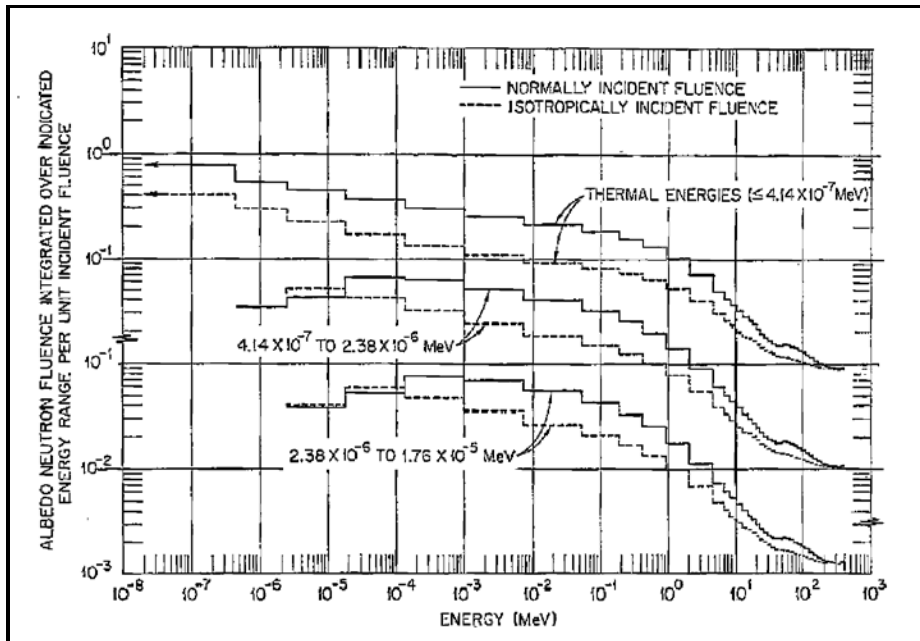


Figure A-4. Albedo-neutron fluence integrated over the specified energy ranges vs. incident neutron energy for monoenergetic neutron fluences normally and isotropically incident on a 30-cm-thick semi-infinite tissue slab (Alsmiller and Barish 1974).

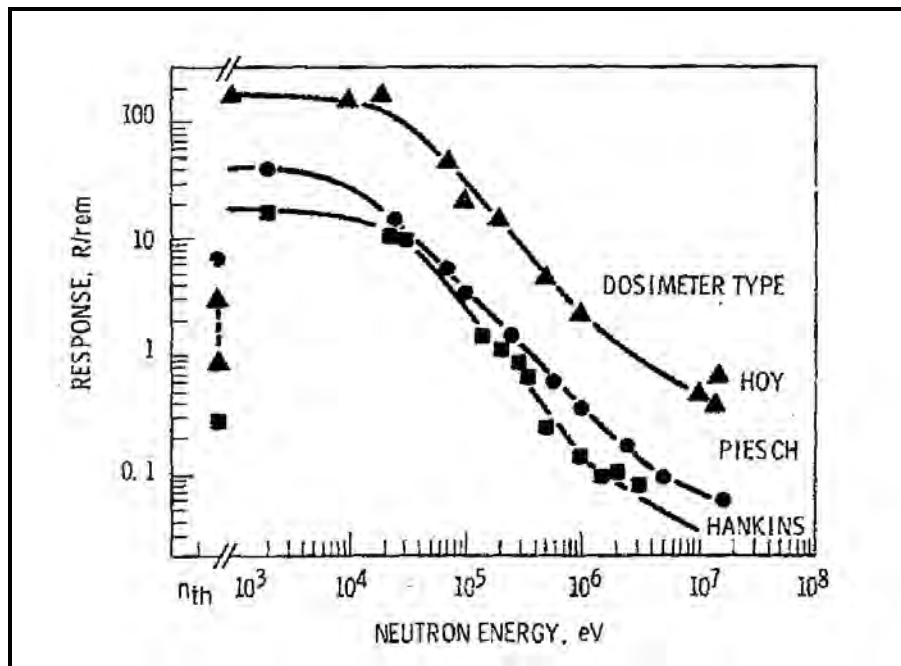


Figure A-5. Energy response of various albedo dosimeters (Piesch and Burghardt 1978).

ATTACHMENT A
HIGH ENERGY TLD NEUTRON DOSIMETRY
Page 8 of 10

cross section and the flux of neutrons as functions of energy. The cross section has a $1/v$ dependence and Alsmiller and Barish (1974) show the flux in three different energy groups for neutrons of different incident energies (Figure A-3). The response to a detector that sees thermal neutrons as well as those above thermal is:

$$R_{SLAC} = R_{Hankins} \left(\frac{\sigma_2 \cdot \Phi_2 + \sigma_3 \Phi_3 + \sigma_T \cdot \Phi_T}{\sigma_2 \cdot \Phi_2 + \sigma_3 \Phi_3} \right) = R_{Hankins} \left(1 + \frac{\Phi_T \cdot \sigma_T / \sigma_2}{\Phi_2 (1 + \Phi_3 \sigma_3 / \Phi_2 \sigma_2)} \right) \quad A-1$$

where σ_j is the average cross section in the j energy group and Φ_j is the fluence in the j energy group. The second term in the denominator is rather small, so it can be neglected. The fluences are shown in Figure A-3, and the ratio of cross sections can be calculated. Figure A-6 shows the Hankins data on the left-hand scale from Figure A-4 (smooth curve), the Alsmiller and Barish calculation for the Hankins dosimeter (1974, Figure 14) in diamonds on the right-hand scale [which agrees well (after a scale adjustment) with the Hankins data], and the results of Equation A-1 shown in squares on the right-hand scale and extending to 1×10^{10} reactions/rem at low energies. The triangles are SLAC calibration data on a phantom (Liu et al. 1991) plotted on the left-hand scale at the mean energy of the calibration spectra. The intermediate histogram on the left-hand scale is an adjustment of the uppermost curve for a detector without cadmium to fit the SLAC calibration data and is appropriate for combining with neutron spectral information to evaluate spectral response of the SLAC LiF TLDs. SLAC documents also quote a response of 150 V/rem for thermal neutrons for unmoderated TLDs not on a phantom (Liu et al. 1991).

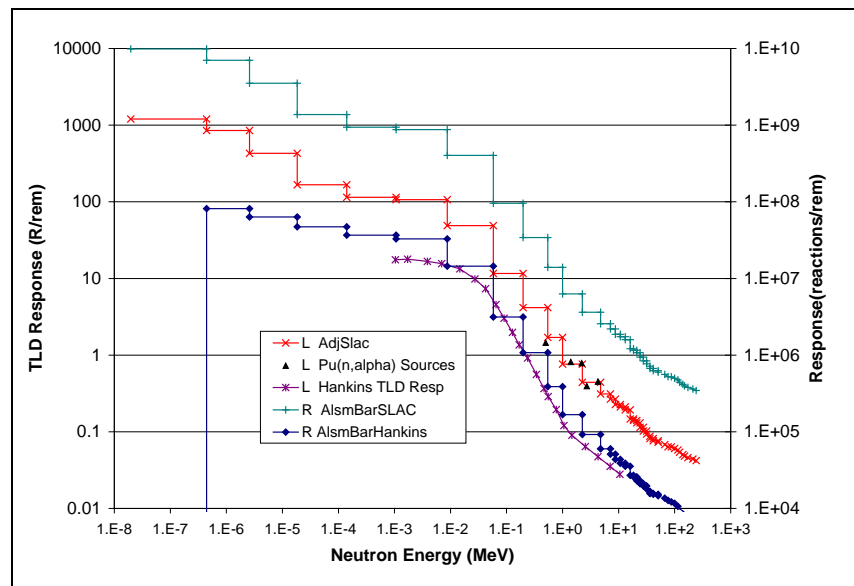


Figure A-6. TLD response for monoenergetic neutrons.

Comparison with the PMS or moderated TLD curve shows that the TLD badge response drops off much faster with increasing energy than does the moderated system. This curve can then be folded onto the high-energy spectra to yield the TLD results shown in Table A-1. Combining the spectral information with the response curve results in response factors of 38.4 V/rem for the SSRL LINAC spectrum, 52.2 V/rem for the SSRL SPEAR spectrum, 5.47 V/rem for the FFTB2 spectrum, 5.90

ATTACHMENT A
HIGH ENERGY TLD NEUTRON DOSIMETRY
Page 9 of 10

V/rem for the CERN iron spectrum, and 3.87 V/rem for the CERN concrete spectrum shown in Table A-1. Although the SPEAR has higher energy neutrons, the TLD response is higher rather than lower because it also has more thermal neutrons. These calculated calibration factors cover a range of a factor of 13.3.

In a similar fashion as the PMS system, one can consider how the conventional Hankins TLDs would respond. Because the response curve for the Hankins TLD in Figure A-6 only goes from 1 keV to slightly above 10 MeV, the calculated response by Alsmiller and Barish (1974) in Figure A-6 was adjusted to cover the low- and high-energy response regions. For the high-energy spectra (CERN concrete and FFTB2) the response is low (0.236 and 0.299 respectively), for the low-energy CERN iron spectrum the value is 0.985. For the SLAC SSRL spectra that have more low-energy neutrons, the values are 1.457 and 1.523 for the SPEAR and LINAC, respectively. The order of the SSRL Hankins TLD responses is reversed because there is no thermal response. Therefore, the TLD response to dose conversion factors varies by a factor of almost 6.5 for these five measured spectra. This range is only about half the calculated range for the SLAC LiF detector, but the signal is reduced by about a factor of 17.5 from the SLAC detector.

Comparison measurements described by Jenkins and Busick (1987) have been made to demonstrate the conservative nature of the LiF TLD calibration. Neutrons existed at several locations around the SLAC Research Yard, particularly in the early days when high-power beams impacted onto fixed targets in one of the End Stations. This could be from leakage through side walls or skyshine due to thinner roof shielding. Bare and moderated LiF TLD monitors were placed in about 25 locations around the Research Yard. The difference in signal between ^6LiF and ^7LiF on a ruler inside the moderator was attributed to fast or moderated neutrons. Mounted on the other end of the ruler, ^6LiF and ^7LiF TLDs measured the ambient thermal neutrons and gamma radiation. A similar system is still in use, some in 5-in. moderators that do not have the cadmium cover and some with Panasonic UD-802 detectors. From these measurements, the ratio of moderated to unmoderated flux has a median value of 2.75 with 80% of the values between 1.6 and 4.4. To generate low-energy neutrons for calibration, a neutron source was placed in a concrete tunnel and the monitors were placed at different distances, which resulted in different ratios of moderated to unmoderated flux. Using four (α, n) neutron sources with various energies and at various distances, the TLD response per millirem was determined versus the ratio of moderated to unmoderated flux. As shown in Figure A-7, the solid curve is the responses of the calibration sources in the tunnels comparing on the vertical, the moderated to unmoderated flux and on the horizontal the TLD signal in millivolts divided by the calibration source neutron dose in millirem. A TLD signal of 1 mV/mrem that was used to state personnel neutron dose would have a moderated to unmoderated flux ratio of 9. For the range of moderated to unmoderated flux in the Research Yard (1.5 to 5), the TLD sensitivity was 1.5 to 4 nC/mrem, so the reported personnel neutron dose would be high and thus should be divided by a factor of 1.5 to 4.

The dose in this case is from a neutron source with maximum energy less than 10 MeV. Assuming that very little to half of the dose is above 20 MeV and essentially does not generate a TLD signal, the range would be from about 0.75 to 4. The spread of this result is not significantly different than the calculated spread of 3.9 to 52 reported in Table A-1 for the SLAC LiF detector. It is not understood why the mean value measured by Jenkins and Busick (1987) is significantly lower than the calculated value for the SLAC system. The mean value is slightly higher than the calculated values for the Hankins detector.

ATTACHMENT A
HIGH ENERGY TLD NEUTRON DOSIMETRY
Page 10 of 10

The neutron dose equivalent for the SLAC LiF system used from 1971 should be reduced by a factor of 1.8 with a GSD of 2.5 [14]. The large uncertainty is likely due to different albedo neutron detector responses to different spectra at SLAC; there was no attempt to evaluate the different spectra to which individuals were exposed. To attempt such an evaluation would have been a time-consuming task that would likely have been unsuccessful. The correction is due to the fact that SLAC conservatively erred on the side of over-reporting the neutron dose equivalent.

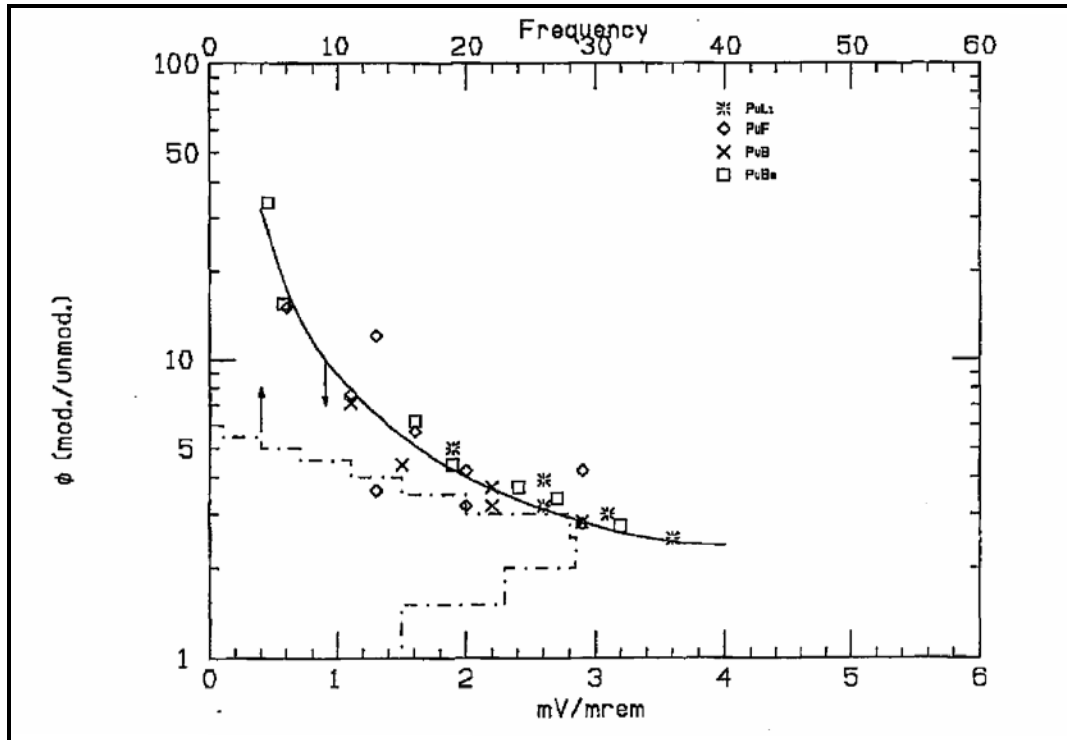


Figure A-7. Sensitivity of TLDs versus moderated/unmoderated flux ratios with research area ratios inscribed.

The Panasonic UD-802 detector used from 1996 to 2001 uses natural $\text{Li}_2\text{B}_4\text{O}_7$ rather than enriched LiF. The TLD signal comes from both the Li and the B and natural material is used. Based on the relative cross sections and the fractional abundances of the isotopes, the ratio of neutron signal to gamma signal for the Panasonic should be about 0.6 that of the LiF. This ratio is substantiated by the relative sensitivity of the two systems in moderators (Liu et al. 2000). We understand that the reported neutron doses for the Panasonic system until March 2000 were based on the unmoderated ^{252}Cf spectrum, resulting in reported doses being about a factor of 7 too large (Flood 1995c).